FRICTION AND WEAR OF POLYETHYLENE IN MULTIDIRECTIONAL MOTION: QUANTITATIVE DESCRIPTIONS OF CURRENT THEORY

By

ALISON C. DUNN

A THESIS PRESENTED TO THE GRADUATE SCHOOL
OF THE UNIVERSITY OF FLORIDA IN PARTIAL FULFILLMENT
OF THE REQUIREMENTS FOR THE DEGREE OF
MASTER OF SCIENCE

UNIVERSITY OF FLORIDA

2006

This document is dedicated to the graduate students of the University of Florida.

Happy is the man who finds wisdom,
And the man who gains understanding;
For her proceeds are better than the profits of silver,
And her gain than fine gold.

-Proverbs 3:13, New King James Version

ACKNOWLEDGEMENTS

I would like to thank my husband Nick for his unending love and unending jokes during my time in school. Great appreciation goes to my family as well, for shaping and guiding me: Robert and Patricia Rennie, Jill, and Russell. I would also like to thank all of my lab mates for their help, advice, and ability to have fun: (in no particular order) Dan and Pam Dickrell, Luis Alvarez, Nicole McCook, Snake Mauntler, Jeff Bardt, Vinny Lee, Jerry Bourne, Benjafriend, Jason Bares, Dave Burris, Matt Hamilton, Nick Argibay, and Jason Steffens.

I would also like to thank the professors who have worked with me on other projects and taken an interest in helping me develop professionally: Malisa Sarntinoranont, Scott Banks, and Tony Brennan. Above all, I would like to thank my committee chair and advisor Greg Sawyer for his friendship as well as welcoming and challenging me into the world of engineering research. Though he is busy, he is often helping others to achieve their goals. I would like to acknowledge MAKO Surgical Corporation for financial support of this work.

TABLE OF CONTENTS

Page

TABLE

LIST OF FIGURES

Abstract of Thesis Presented to the Graduate School
of the University of Florida in Partial Fulfillment of the
Requirements for the Degree of Master of Science

FRICTION AND WEAR OF POLYETHYLENE IN MULTIDIRECTIONAL MOTION: QUANTITATIVE DESCRIPTIONS OF CURRENT THEORY

By

Alison C. Dunn

August 2006

Chair: W. Gregory Sawyer
Major Department: Mechanical and Aerospace Engineering

Multi-directional wear of UHMWPe is of particular interest due to its use as the state-of-the-art bearing component polymer in orthopaedic implants. In unidirectional sliding, UHMWPe chains or fibrils are able to align on the surface forming a stable, low shear running film which leads to very low rates of wear. During directional changes, these running films are disrupted, and additional energy is required to align the chains in the new direction of sliding, during which some of the chains may break off as wear debris. When this process takes place briefly in a wear path, a higher local friction coefficient results. In addition, when the process repeats continuously over the entire wear path, a higher average friction coefficient results. It was hypothesized that *in situ* friction measurement over a relevant motion path will give a better understanding of the relationship between friction and wear. A custom-built multidirectional tribometer was built to supply uniform velocity and pressure under the contact, some characteristics absent from current modeling of the theory described above.

Friction is observed as a function of parameters of a curvature-modulated wear path (radius of curvature $\rho = 1 – 1400$ mm). In general, the spatially resolved friction coefficient increased with decreasing ρ of the sliding path, which is consistent with some orientation of the surface. Previous models are used to predict the change in friction coefficient as the wear path curvature changes. These predictions are used to verify the hypothesis that friction in multidirectional sliding is directly correlated to the UHMWPe surface orientation, which leads directly to wear.

CHAPTER 1
INTRODUCTION

Orthopaedic implants are becoming increasingly common for younger patients, and the finite wear lives of these joints require multiple surgeries to carry patients through long life. Consequently, the state-of-the-art bearing material, ultra-high molecular weight polyethylene (UHMWPe), has been the focus of a significant number of research efforts aimed at improving the lives of these implants. Creep, counterface roughness, third body wear, and sensitivity of the material to multidirectional motion paths have all been cited as primary contributors to premature bearing failures in UHMWPe implants.

Orthopaedic Implant Development and Research

In the earliest knee replacement, engineers used an unnaturally over-constrained mechanics model; in the 1970s, Install's Condylar Knee was used with wide success, though high wear. Later innovations reduced wear and allowed more of the natural ligaments to stay in place. Today, the modular total knee replacement (TKR) has had great success in restoring the quality of life to those with knee impairments (Figure 1-1). The key element of a TKR is the load-bearing polyethylene that functions both as a support and a solid lubricant. Paradoxically, this key component is also the cause of failure because the forces applied over time cause wear and degradation.

Many researchers have taken clinical retrievals of these bearing components to study the wear and deformation that occurred during the life of the bearing [1-5]. This wear is well-quantified on the order of millimeters per year thickness worn away. Specifically, Fregly, Hamilton, and Laurent used the geometry of clinical retrievals along

with other tools such as *in vivo* observations and finite-element methods to map out wear rates and the motion path seen on the UHMWPe bearings in particular cases [3-5].

Friction and Wear in TKR Bearings

It is well accepted that higher sliding friction produced between UHMWPe and a metal surface will produce more wear of the polyethylene. Friction tests are one of the primary ways to assess the effectiveness of treatments on UHMWPe such as irradiation or absorbed fluid. Various unified theories of polyethylene interactions include friction, wear, material, and physical considerations, but all must assume constant friction coefficient or constant velocity to allow other parameters to be fit to empirical data. This thesis work entertains the suggestion that friction measure over the course of a motion path can more adequately give an indication of the mechanisms of wear, not just a gross observation of wear over a specified interval. The motivation for this work is an incomplete treatment of the coupled mechanisms of friction and wear of polyethylene. The goal of this work is to improve unified wear theories in scope of applications and accuracy. Relevant experiments were devised and executed to explore the friction traces of various multidirectional motion paths, as well as to discuss the pertinence of the results to the current unified theories.

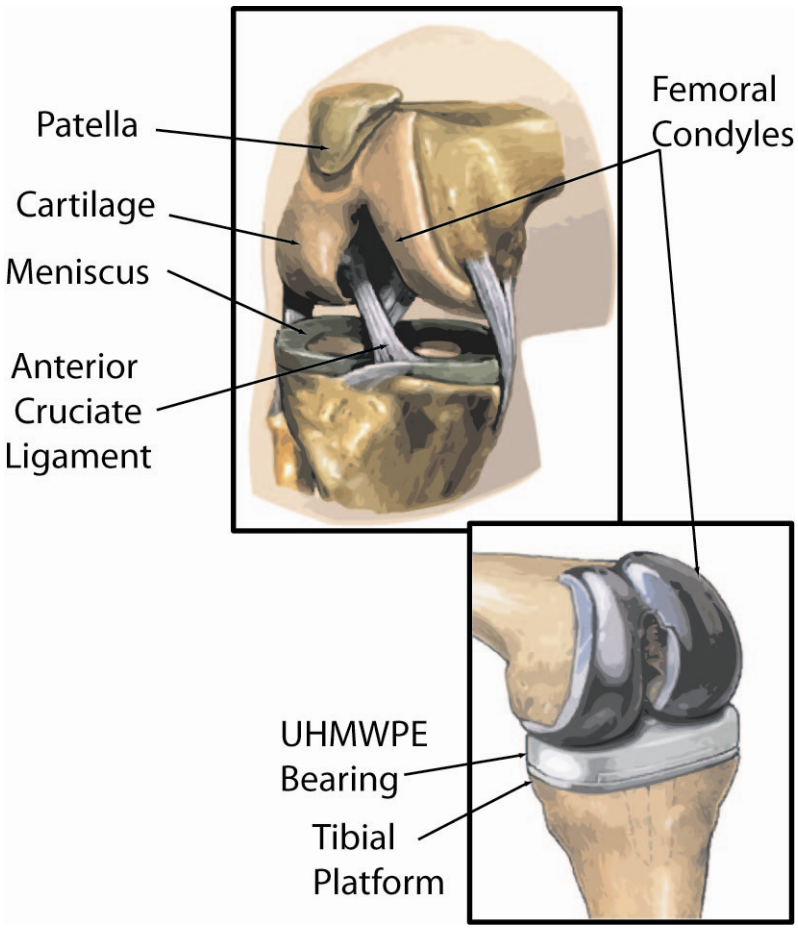

Figure 1-1. Drawing of knee anatomy and anatomical changes with a total knee replacement.

CHAPTER 2
MOLECULAR ORIENTATION HYPOTHESIS

This chapter discusses the current theory of molecular chain orientation in special polymer samples while in sliding contact. The experiments to verify this hypothesis are very new, and include work from industry and academia.

Ultra-high Molecular Weight Polyethylene (UHMWPe)

Many materials including metals, ceramics, and polymers (plastics) have been examined for possible use in the human body, especially for bearing components in partial or total joint replacements. The current state-of-the-art total knee replacements use metal components that attach to the femur and tibia bones with a polymer bearing, essentially a slab, between them made of ultra-high molecular weight polyethylene (Figure 2-1).

The metal components are typically cobalt-chromium-molybdenum alloys (CoCr), and the polymer is typically ultra-high molecular weight polyethylene. This "special engineering polymer" was chosen for many reasons: it is biologically inert, easy to manufacture, has low friction and wear, and is very durable. In conjunction with the synovial fluid of the knee, this polymer can function in a TKR for up to 15 years should the patient remain trim and only moderately active.

UHMWPe is a semi-crystalline polymer. Upon processing, it crystallizes as it cools. It has been reported that UHMWPe can be cross-linked before or after molding. UHMWPe is less likely to wear if cross-linked because there are more bonds holding the chains together, limiting polymer chain scission.

Performance of UHMWPe in Sliding

The over-arching theory is that when the polymer deforms in sliding, some geometry of the polymer like fibrils or molecular chains orient themselves along the direction of sliding, and then either break off or re-orient when the motion changes direction, whichever requires less energy. The most appropriate way to describe this change in motion is an angle α that is calculated as a velocity vector change due to coupled rotation and linear sliding motions (Figure 2-2). Previous work shows that UHMWPe performs well in both dry and lubricated sliding. Author Gonzalez-Mora has shown that since this polymer is so compliant in comparison with its counter-surface, the exact constitution of the CoCr alloy is negligible [6].

In dry sliding, UHMWPe forms a thin transfer film on the counter-surface which allows for polymer-polymer sliding. These low-shear running films are formed from surface defects or high pressure causing polymer chains to be pulled into the contact and semi-permanently transferred to the counter-surface. When these chains collect and cover the contact area, the friction is lowered because the polymer is sliding on an oriented layer of chains with the same molecular composition rather than sliding on the initial wear surface (usually metal or ceramic). Even in initial sliding of a friction experiment, there can be surface orientation of the pin though no material has yet visibly transferred to the counter-surface, and therefore stable friction can be disrupted before a transfer film has formed.

In lubricated sliding, fluid particles such as water fill small spaces within the contact and prevent this transfer film from forming. However, friction and wear in the presence of lubrication remain low if the both the polymer surface and the sliding counter-surface are very smooth (R_z ~ 5-10 nm). The primary wear mechanism of

UHMWPe is commonly referred to as delamination, which means the wear particles are thin patches released by cracking due to subsurface shear stress (Figure 2-3). That debris helps form the transfer film, or is pushed free from the contact zone. Authors have used friction and wear to screen different types of UHMWPe, whether it has been modified by irradiation, cross-linking, or additives. Some have also used other techniques such as a punch to deform the materials. Delamination or other wear debris as well as the wear surfaces are analyzed in detail with scanning electron microscopy (SEM) [7-11]. These techniques are very appropriate given consistent loading and velocity conditions.

Current Surface Orientation Hypotheses

Three main research groups have developed testing machines and subsequent theories about how to describe this surface orientation for their particular setup, and how it is manifest in friction and wear data.

Stryker Howmedica Osteonics: Dr. A. Wang

Dr. Wang's theory takes the perspective of a general orientation of the polymer surface and defines from that a geometry of wear debris. This stems from the assumption that there is a preferred orientation direction, in which energy is dissipated in chain motion, but does not contribute directly to wear. Following from this is a perpendicular direction in which chains (and cross-links) are broken apart from each other, causing elongated fibril-shaped wear debris (Figure 2-4). Energy in that direction does not include chain motion but bond rupture, and contributes directly to wear. Based on bond strengths and the work to remove a single fibril, a wear equation was developed (Equation 1),

$$k = k' \frac{d\left(\mu - \mu_0\right)}{2\gamma_c}\left(M_c - M_0\right)\left(1 - \frac{\sin 2\alpha}{2\alpha}\right) \qquad \text{Equation 1}$$

where k' is a wear rate constant, μ is friction coefficient, γ is the C-C bond energy, M_c is the average molecular weight between crosslinks, M_0 is the critical molecular weight between crosslinks, and α is the cross-shear angle. This is multi-parameter model that is born from the wear geometry assumption; the relationships between variables have been verified, but the model as a whole has yet to fully describe a system. The apparatus used to perform the experiments was a custom-built simulator where rotation is applied by a top component (polymer pin), and linear reciprocation is applied by the flat plate (metal counter-surface) [12]. Of particular interest is the added term μ_0 which describes the initial friction coefficient. This means that wear is related to a rise in the friction coefficient due to this fibril orientation.

Clemson University: Martine LaBerge

This group has built an apparatus with x- and y-tables that can be simultaneously controlled, providing multi-direction path capabilities to their UHMWPe plate sliding against a spherical steel pin. They perform 5 tests with the same motion path, a 5-pointed star with 5 crossing points. They compare this to the motion seen by the tibial component in TKRs, but neglect curvature of the motion path. They conclude that there is a direct and quantitative relationship between the measurements of cross-shear angle and linear damage, and that the ratio of those measurements is indicative of a material's ability to resist wear in a cross-shearing configuration [13].

University of Leeds: John Fisher

This group uses similar equations to Dr. Wang, but they also map out discrete locations on the pin surface to track during their test (Figure 2-5). They recognize the velocity distribution and calculate an average cross-shear ratio under the pin contact. Their conclusions are as follows: a) during unidirectional sliding, an orientational

'hardening' of molecules occurs along the sliding direction; a 'softening' in the perpendicular direction, b) cross-linking increases bonding, retarding chain mobility and resisting breakage, and c) cross-linking provides less orientation hardening because the molecular chains cannot move as much, and therefore a lower wear rate [14].

Crosslinking

Conflicting conclusions regarding how crosslinking affects this surface orientation theory are present in current literature. Authors Galvin [14] and Muratoglu have concluded that "crosslinking inhibits this important mechanism responsible for wear, i.e. orientation and re-orientation …" [15]. Conversely, Author Kurtz affirms that "both radiation and chemical crosslinking hinder molecular mobility at large deformations, and hence promote strain hardening and molecular alignment during the multiaxial loading of the small punch test" [8].

New Hypothesis: Friction Trace Insight

All manifestations of this theory so far agree that cross-linking helps to make an UHMWPe component more wear resistant, and generally agree that chain elongation and rupture are the mechanisms that lead to failure. This work probes this theory by inspecting in situ friction traces of multidirectional motion paths. Friction coefficient is an indication of energy needed to put two surfaces in relative motion, so changes in energy dissipation caused by surface orientation and re-orientation should be discernable. It is presumed that the friction trace can also be used not just to surmise that more friction leads to increased wear, but that specific locations of increase are causing some higher percentage of wear than other locations. The ideal experimental set up would measure wear in situ for a variety of locations along a motion path. The final way a friction trace would influence understanding of UHMWPe wear is that friction as a function of either

path geometry can be inserted into a unified wear theory. The aim of this work is to show how in situ friction measurements can inform surface orientation theory, wear prediction, and unified theories of sliding wear of UHMWPe.

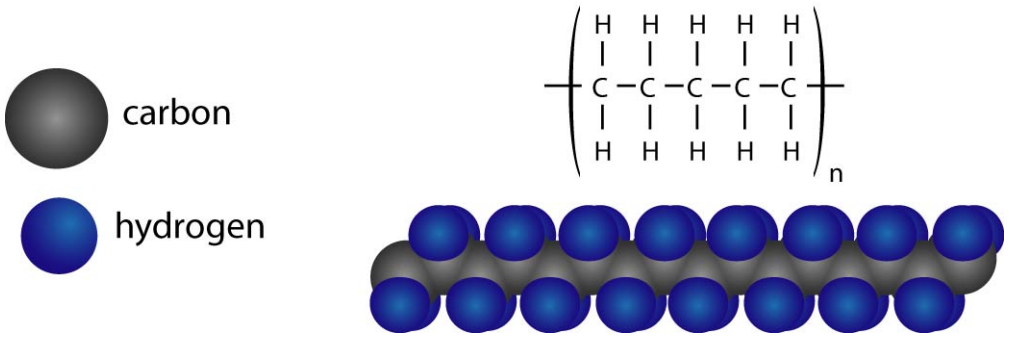

Figure 2-1. Molecular structure of UHMWPE.

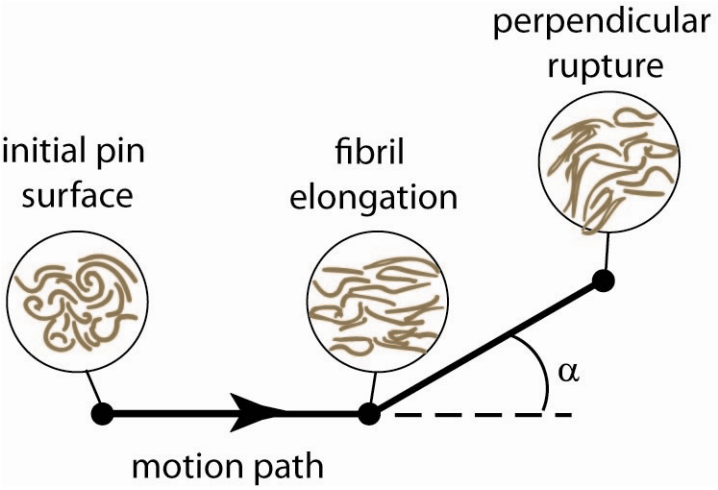

Figure 2-2. Schematic of fibril orientation and rupture on surface of UHMWPE pin as it moves along a non-linear motion path.

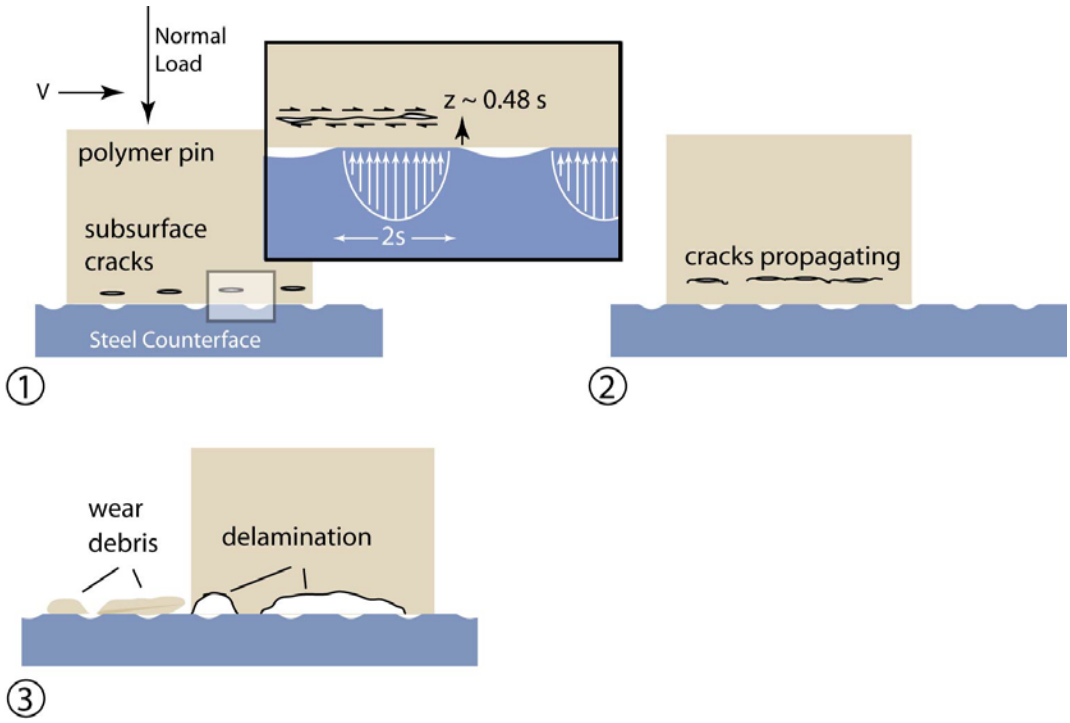

Figure 2-3. Schematic of the delamination wear of polyethylene in dry sliding.

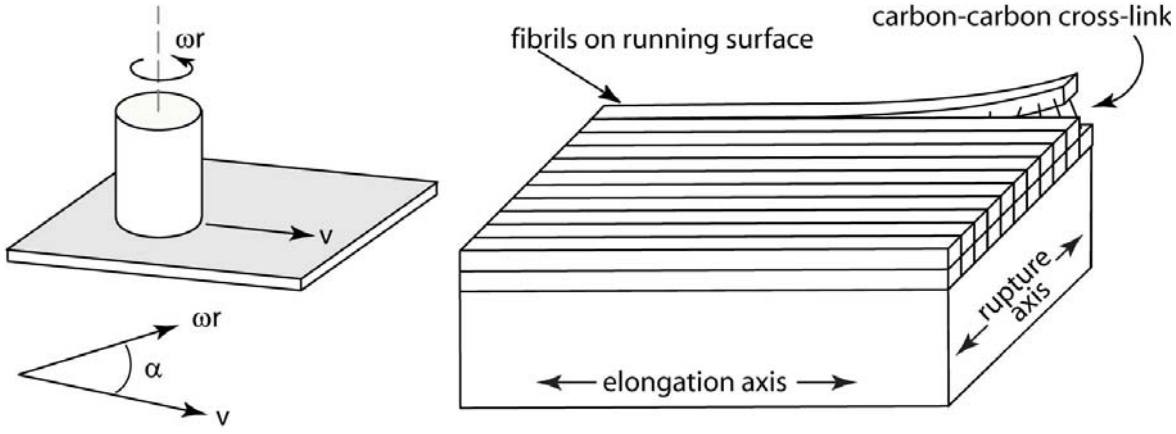

Figure 2-4. Schematic of the two-component experimental setup and a schematic of the wear theory with fibril elongation and perpendicular crosslink rupture.

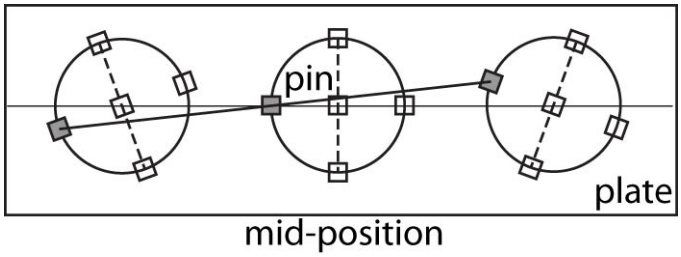

Figure 2-5. Schematic of motion of a single point on a rotating and translating motion path.

CHAPTER 3
EXPERIMENTAL SETUP

Friction Coefficient Measurements

Friction coefficient is defined as the friction force produced divided by the normal force applied (Figure 3-1). Because of this, tribometers must be designed with force reaction paths as the foremost consideration, as friction measurements should be made with the highest resolution available in order to illuminate subtleties.

Friction is typically measured with a load cell, so there must be no other ways to react the friction force outside of the load cell. Motors and stages cannot be frictionless, so the load cell is not able to be fixed to the component that provides motion to the tribometer contact. The apparatus designed for these experiments uses an AMTI 6-channel load cell mounted to pneumatic thrusters, which apply a normal load. The sample pin is mounted directly to this load cell (Figure 3-2). Two Parker ball screw stages are mounted to the table perpendicular to each other, which provide two-axis motion to the counter-sliding surface (Figure 3-3). Therefore, when the stage moves, all forces produced in the contact are reacted up through the sample and in the load cell. One key feature of this tribometer is that all points under the pin have the same velocity and pressure – this is achieved by keeping any rotation and linear sliding in the linear path coupled together. Other authors have achieved this as well [13,15,17-21]. This entire setup operates in a class 10,000 clean room under slight positive pressure to prevent ambient contamination.

Multi-directional motion can be produced a variety of ways, from cams to linear motors. For this work ball-screw linear motors were utilized because they are capable of 50,000 pulses per revolution, up to 2 in/sec. Motion paths are created by uploading a Microsoft Excel file that interfaces with the master LabView program. To assure a continuous path, splines are created from the ideal excel file. This master program both runs the experiments and measures the outcomes in a usable format.

Other tribometers that have been used to create 'multi-directional' motion have used components that necessitate a variety of assumptions which confound data analysis and theoretical application. For example, Dr. Wang's apparatus that others have copied uses a rotating pin in unidirectional sliding [14, 22-24]. In this way, his simulator has separate rotation and linear sliding components, considered a relevant setup for hip replacement motion. However, because those motions are decoupled, the velocity under the rotating pin is not constant and varies radially (Figure 3-4). The faster-moving outside edge will dissipate more energy, and therefore wear more.

After this happens, the pressure under the contact is non-uniform and increases over the course of a test as the contact area decreases. In the course of his analysis, pressure is assumed to be constant, causing errors in the range of values to which his other parameters can be fit. One might argue that the pressure does not deviate enough over the course of the test such that it cannot be considered 'constant,' but the complications of applying theories of fibril elongation and rupture still exist. If the surface of the pin elongates the fibers in such a way that they are circles of constant radius emanating from the center of the pin, it is impossible to determine and model a single sliding direction of the pin that would be perpendicular to that. This non-uniform

velocity and pressure do not allow the apparatus results to apply appropriately to UHMWPe wear in TKR bearings. One last apparatus possibility for providing multidirectional motion is a commercial knee or hip simulator. Authors Fisher and Turell have explored this option [25-27], with the latter attempting to get rectilinear motion by matching the rotation of both counterface and pin on a commercially available OrthoPOD pin-on-disk by Advanced Mechanical Technology, Incorporated (AMTI).

Sample Preparation

UHMWPe used for this work was provided by the Hospital for Special Surgery in New York City. From this sample, cylinders 0.2 inches in diameter and 0.3 inches long were cut using a programmable Minitech Machinery Corporation CNC milling machine. The running surface of the sample was prepared by slicing one face with a razorblade. The provided has a molecular weight of approximately 6 million.

Cobalt-chromium-magnesium (CoCr) counterfaces were obtained from Encore Orthopaedics and were polished to an RMS roughness of 5-10 nm on a polishing and lapping wheel. The disk was then adhered to the plate mounted to the linear stages.

Test Parameters

The testing conditions varied based on the limitations of the apparatus to hold bovine serum and maintain a full range of motion. Table 3-1 lists the various test parameters. Bovine serum is a constituted of 25 mg/mL protein from Hyclone Alpha Calf Fraction and 0.3% EDTA as a preservative. Anti-bacterial agents such as sodium azide are omitted due to possible hazards.

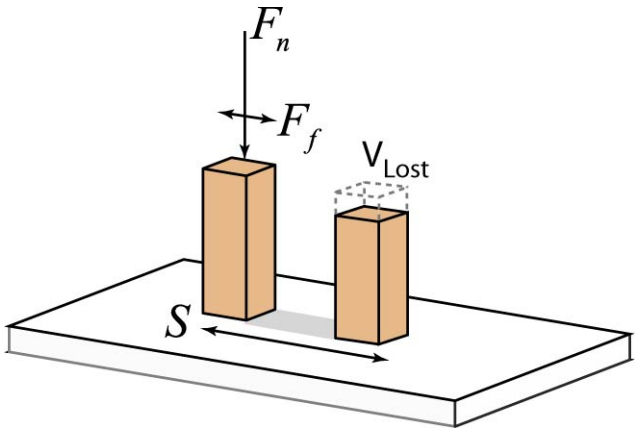

Figure 3-1. Schematic of a block sliding on a flat with frictional and normal forces indicated, as well as motion path length and volume lost.

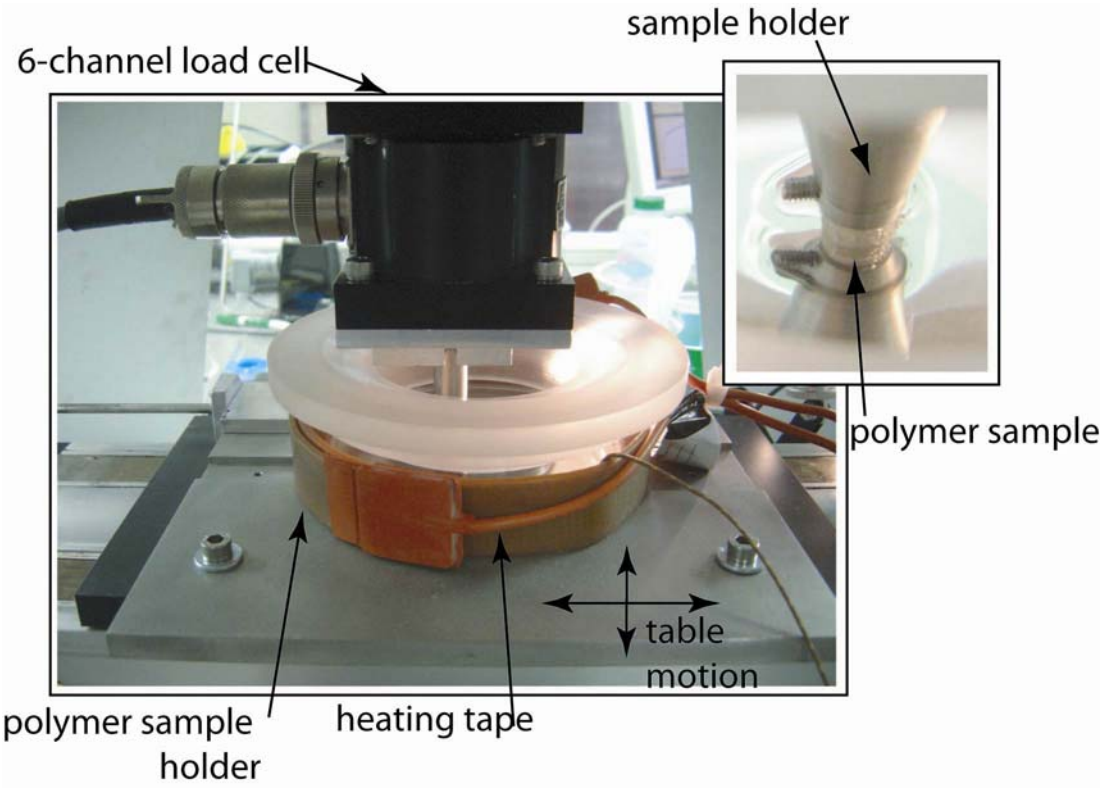

Figure 3-2. Photograph of pin-plate contact including bovine serum bath, heating tape, and load cell.

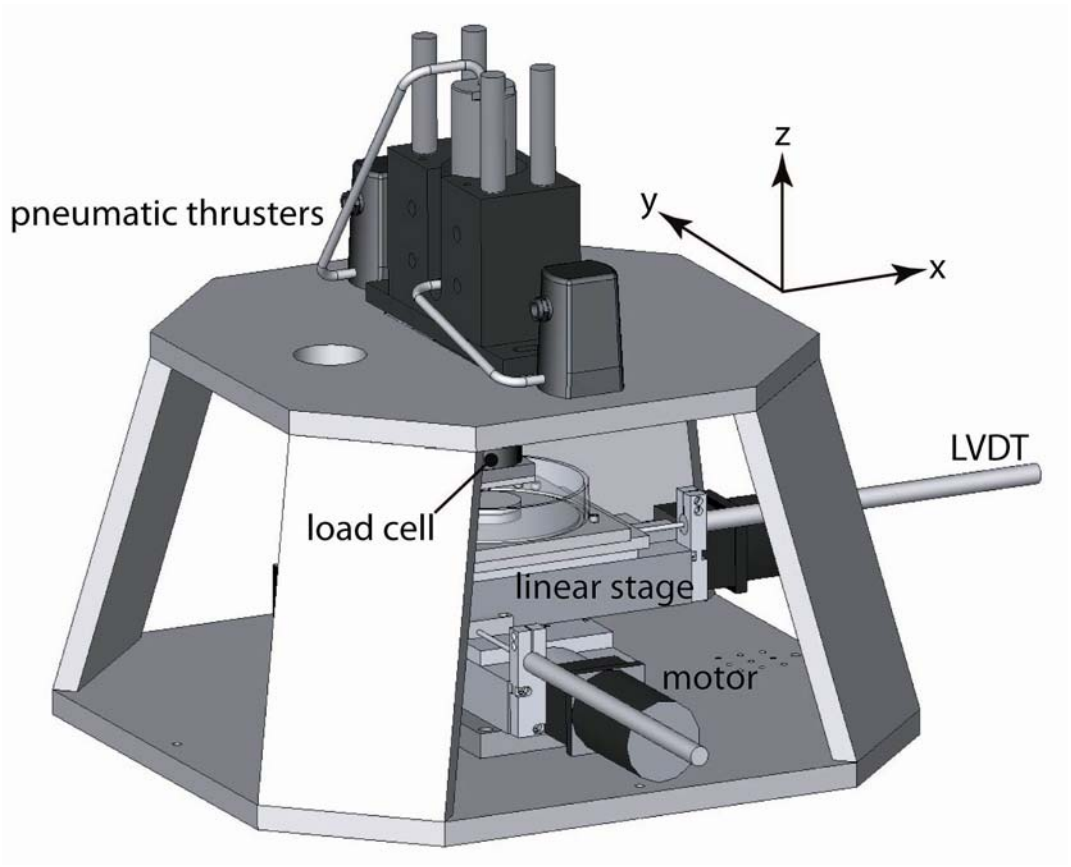

Figure 3-3. Schematic of multidirectional tribometer including linear stages, motors, thrusters, and frame. Courtesy of Jason Steffens.

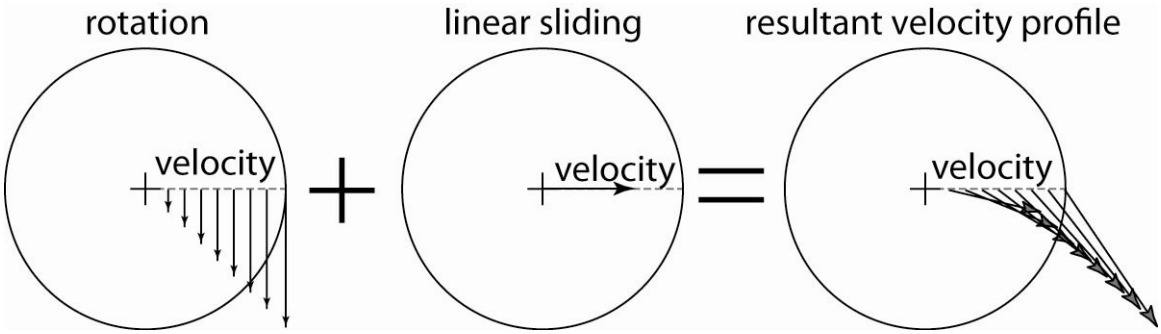

Figure 3-4. Schematic of rotation and linear sliding producing a non-uniform velocity profile on pin surface.

Table 3-1. A list of the test parameters for each motion path run.

Geometry of wear path	size	Lubricant?
Line	50.8 mm	No
Reciprocating circle	50.8 mm	No
Lemniscate (figure 8)	50.8 mm	No
“chirp”	50.8 mm	No
Double Fermat spiral	50.8 mm	No
line	25.4 mm	Yes
lemniscate	25.4 mm	Yes
“chirp”	25.4 mm	Yes
Archimedes’ incr. radius	162.2 mm	No
Archimedes’ decr. radius	162.2 mm	No

CHAPTER 4
MOTION PATHS

This chapter describes the motion paths run on the multi-directional tribometer and discusses the motivations and advantages of each.

Preliminary Motion Paths

Perpendicular ball screw motor linear tables have the ability to run any desirable wear path, so motion parameters were considered carefully. Previous work by an undergraduate researcher was used as the basis for more complex paths[1]. In his work, a simple dry sliding linear reciprocating path was examined with UHMWPe pins as previously described on a CoCr disk to validate the ability of the apparatus to produce wear rates seen by other researchers on these materials (k = 1 x 10^{-7} mm^3/Nm). Next a reciprocating circular path was used due to its dissimilarity to a reciprocating linear path, in that it avoids linear sliding. After this, a lemniscate was examined because it has a single crossing point, along with curvature and a non-uniform aspect ratio. These tests were run up to 1 million cycles and comparative wear of the paths with varying complexity were analyzed. Friction as a function of time was also analyzed, to see if the data supported a link between friction response and eventual wear response of a particular material. The tests were run at 50.8 mm/s sliding speed under 10 MPa of pressure, as this is considered to be an average pressure seen on bearings in TKRs.

[1] Rizwan Sajan ran these experiments in our laboratory on this testing equipment, but the data required analysis before use in this manuscript.

The results of these friction tests show that friction increases over time for all motion paths. Friction is higher for the more complex path shapes because they are constantly changing direction, and it is presumed that the material does not have time to recover (Figure 4-1).

Results also show that over time, the reciprocating circle and reciprocating lemniscate have a higher wear rate and friction coefficient than the linear reciprocating sliding (Figure 4-2). The specifics of the wear rate calculations are described in Appendix A. These results show that higher friction coefficients in multi-directional dry sliding are indeed linked in some way to the overall wear of the materials under identical velocity and pressure conditions. This supports the assertion that the material wears more severely when the surface of the polymer moves in a motion deviates from reciprocation. Because the only testing parameter changed was the motion path, it must be that the surface responds to changes in direction, and therefore must have some sort of directionality itself. These data suggest that the surface cannot recover from the motions that deviate from a line, and therefore dissipates more energy and wears at a faster rate. This is the motivation to devise a motion path that includes all features seen in the clinical retrieval: turnarounds, high aspect ratio, and a variety of curvatures.

Motion Paths

The motion paths seen by TKR bearings are often complex, including high aspect ratios, stop points, turnaround points, and a wide range of curvatures and changes in curvature [16]. Though work has been done to ascertain the typical motion path in TKRs, experimental testing is done with more regular paths that can be reliably reproduced and more easily analyzed. The majority of tribological experiments performed on UHMWPe are reciprocating sliding experiments, in which the polymer pin

slides back and forth over the same path in a straight line. Those experiments can help to distinguish between candidate orthopaedic bearing materials, but are too simple to provide analogous wear mechanisms of polyethylene in an implant bearing situation. The next iteration of testing moved from reciprocating linear sliding to unidirectional linear sliding in a pin-on-disk apparatus, in which the counterface is rotated under a pin mounted at some fixed radius from the center of the disk counterface. This motion is more relevant because it does not include 180-degree changes in motion every cycle; however, that is its downfall as well: it has no turnarounds or stops, as empirical data suggests in TKR (Figure 4-3). Author Hamilton, et al through in vivo kinematic observations and post-mortem analysis of the UHMWPe bearing determined the probably motion path of highest pressure, including velocity [4].

Later work approaches clinically relevant motion paths with the help of cams and motor-driven tables, and proposes multi-directional shapes such as circles [17-18], ovals [19], footballs [20-21] or 5-pointed stars [13]. All of these shapes have merit, but are not complex enough to capture subtle characteristics of a motion path as seen in clinical retrievals.

Initial Complex Motion Paths

Based on the first experiments with lemniscates and their motion flexibility, the more complex "chirp" signal was comprised of lemniscates of various aspect ratios superimposed at $\pi/6$-radian angles until the wear path completed to 2π radians (Figure 4-4). This is called a "chirp" signal because its curvature modulation is analogous to the frequency-modulated signal commonly used in acoustics that sounds like the chirp of a bird. The radius of curvature of the path ranges from 1 – 1400 mm, and it contains some abrupt changes of direction at the center where the lemniscates are oriented differently.

The highest derivative of radius of curvature is 3400 mm/mm. High aspect ratio is achieved by including a long, lean lemniscate with length to width ratio of 14:1.

The motion changes of the chirp path tend to be abrupt, so another motion path was chosen for its gentle changes in radius of curvature over time: a double Fermat Spiral, or parabolic spiral. The radius of curvature on this signal varies from 1 - 40400 mm and the highest spatial change in radius of curvature is 101000 mm/mm. Each motion path has a histogram of position vectors, with higher concentrations along various axes (Figure 4-5).

Archimedes' Spirals

To validate the hypothesis that friction coefficient is drastically affected by a change in motion path curvature, a motion path was examined called an Archimedes spiral. It is unique because motion takes place in one direction on the spiral, allowing the radius of curvature to be either ever-increasing or ever-decreasing, with a straight line return to the start in both cases (Figure 4-6). If the friction coefficient shows some correlation to change in motion path curvature in simpler tests, it will be magnified in tests that isolate the increasing or decreasing radius of curvature.

These paths have a range of radius of curvature of 1-9700 mm. The change in curvature reaches a maximum at 785000 mm/mm. The range of radius of curvature and range of the spatial derivative are shown in Figure 4-7 and 4-8, respectively. These motion paths were run at the same basic parameters as the previous tests: sliding velocity 50.8 mm/s and pressure of 6 MPa. These specific motion paths encompass the range of features observed in the bearings of TKRs, thereby giving pertinent friction results. Also the Fermat and Archimedes' spirals provide isolation of the specific characteristics of gentle curvature and monotonically increasing or decreasing radius of curvature.

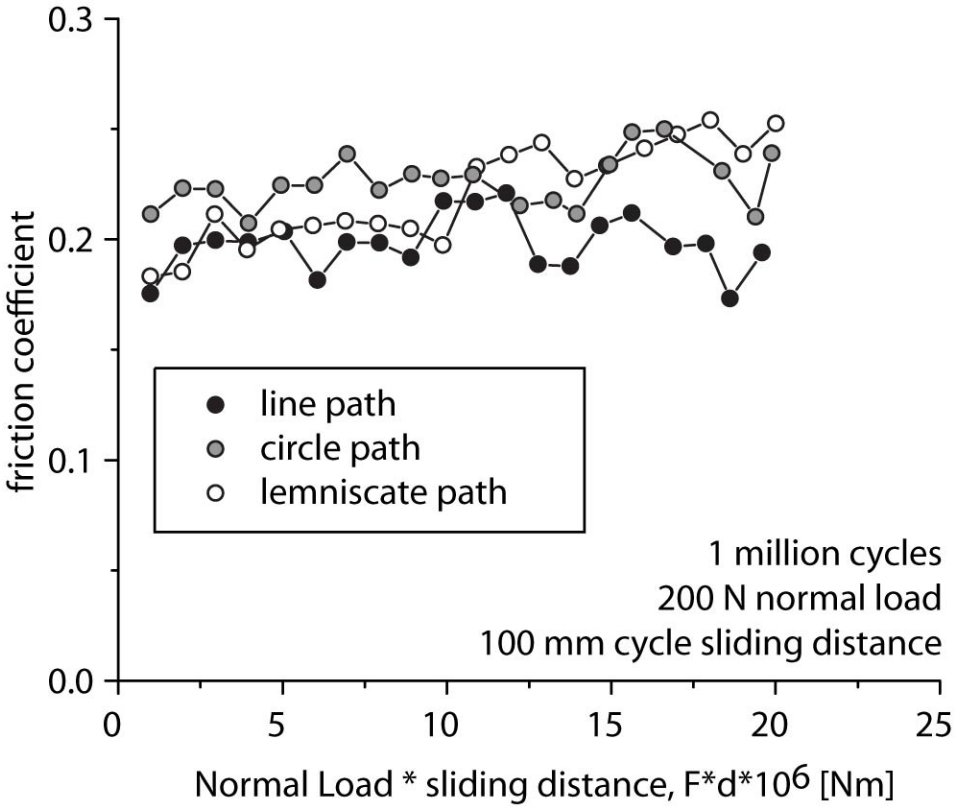

Figure 4-1. Friction results over time for dry sliding of 3 simpler motion paths: line , circle, and lemniscate.

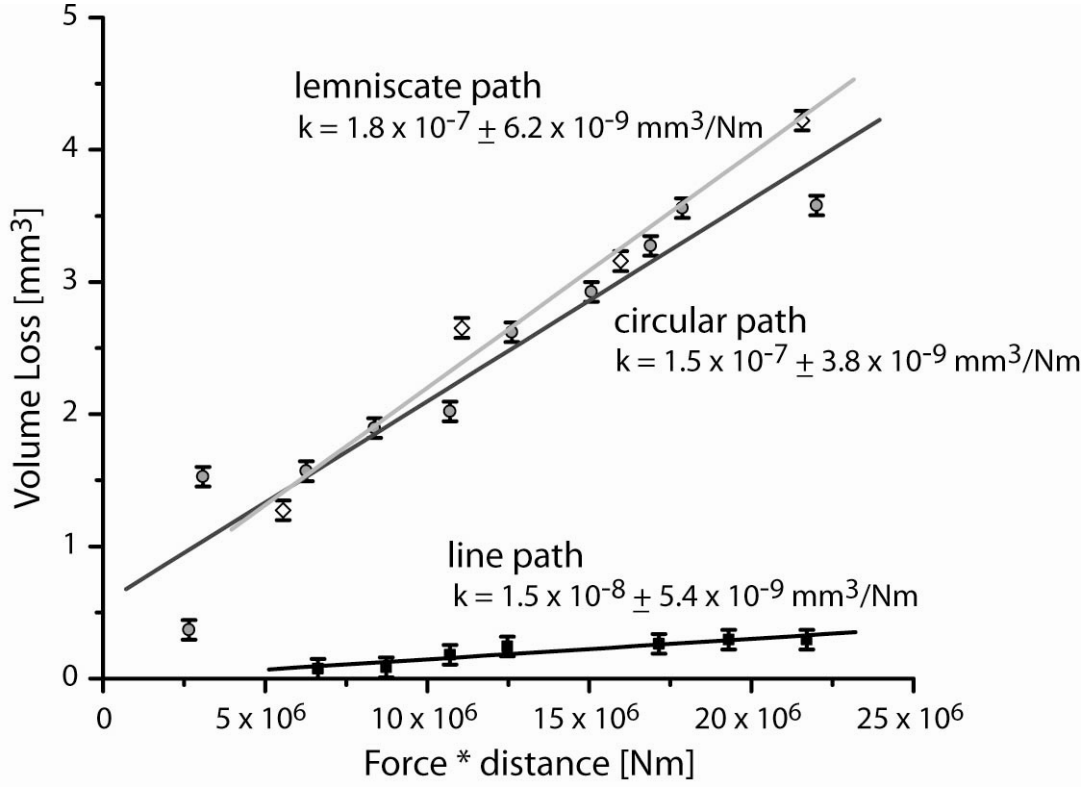

Figure 4-2. Calculated wear rates as the slope of the lines on a plot of volume loss vs. applied force times sliding distance for three simpler motion paths: line, lemniscate, and circle.

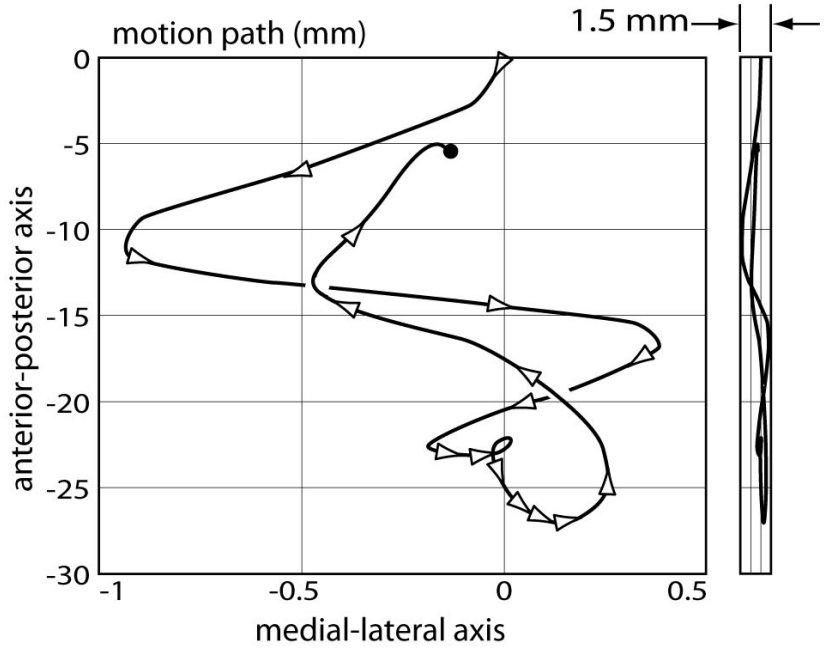

Figure 4-3. Motion path of clinical retrieval UHMWPe bearing based on *in vivo* observations and advance motion mapping.

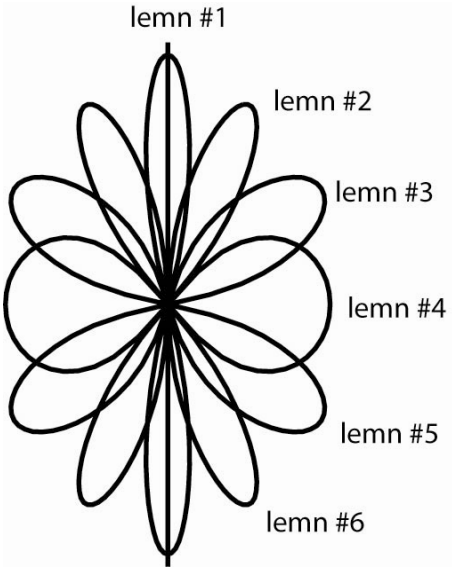

lemniscate	aspect ratio
1	14 : 1
2	10 : 1
3	5 : 1
4	2 : 1
5	5 : 1
6	10 : 1

Figure 4-4. Chirp motion path description with aspect ratio of each lemniscate from 2:1 up to 14:1.

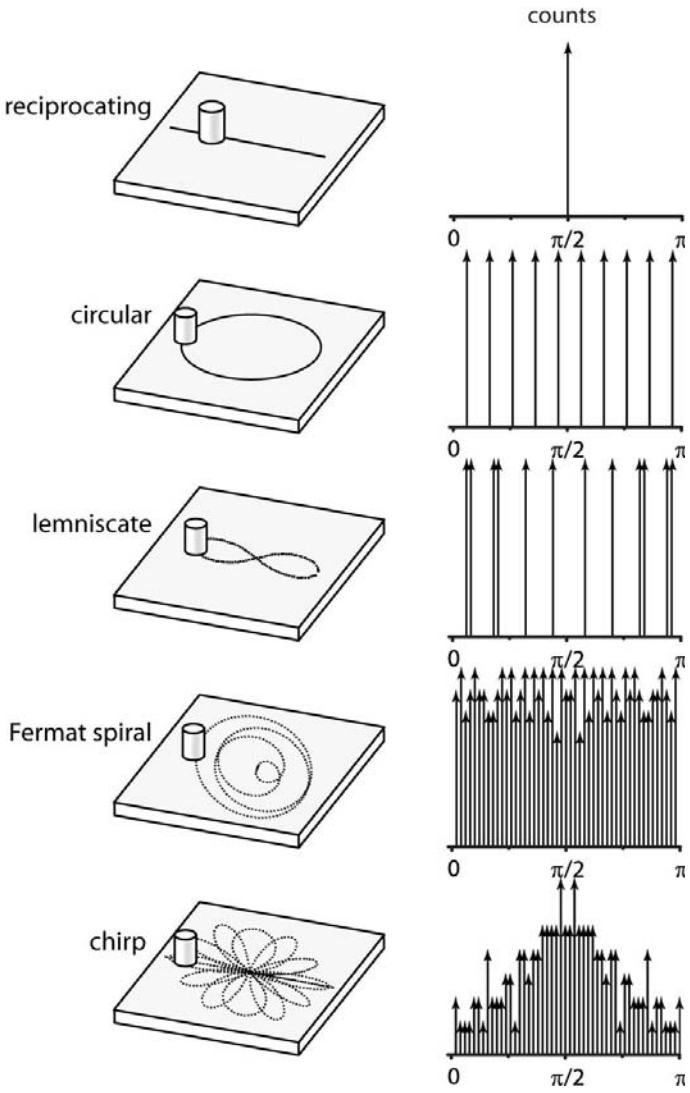

Figure 4-5. Motion paths and relative concentrations of motion direction shown as a histogram of displacement vectors.

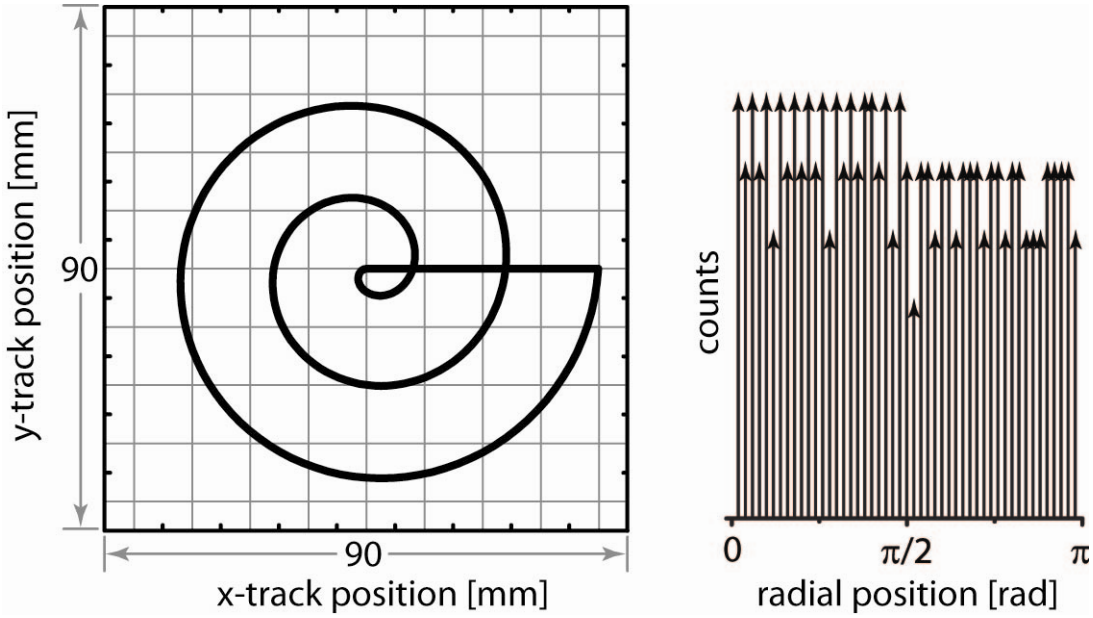

Figure 4-6. Archimedes spiral wear path with ever-increasing or ever-decreasing radius of curvature its motion intensity histogram.

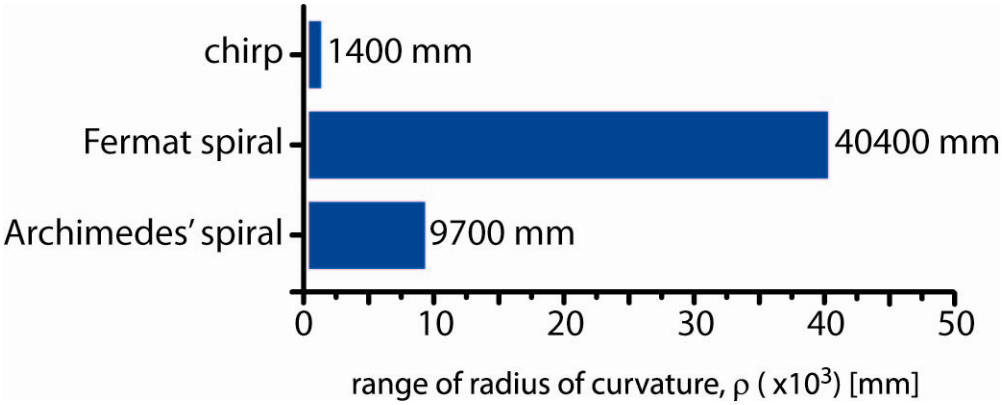

Figure 4-7. Range of radius of curvature for chirp, Fermat, and Archimedes motion paths, in the range of millimeters up to meters.

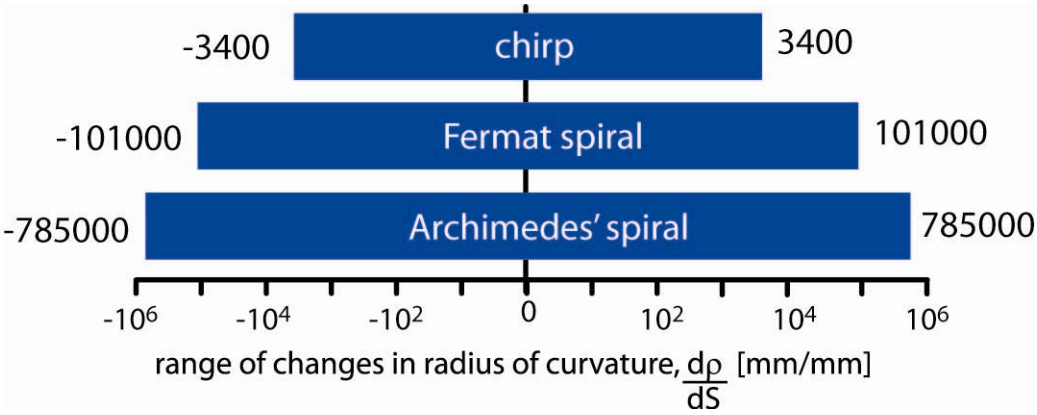

Figure 4-8. Range of change of radius (spatial derivative) of curvature for each motion path

CHAPTER 5
FRICTION RESULTS

Complex Motion Path Friction Results

A plot of average friction coefficient over 100 cycles of sliding plotted versus relative motion path complexity shows that friction is increased for more complex path shapes (Figure 5-1). For each path, 2-D friction color maps were plotted to facilitate spatial geometry observations with respect to friction. This was done by taking the 3-D plot of x-position, y-position, and friction coefficient, then mapping the latter axis down onto the x-y plane with different colors to indicate levels of friction coefficient measured (Figure 5-2). The results from a single dry sliding curvature-modulated "chirp" cycle show that friction increases from the start point of the cycle (path length s), then fluctuates with each lemniscate loop before the end of the wear path.

One trend is the increase in friction at the tip of each lemniscate leaf, specifically an increase in friction when entering the curve, and a subsequent decrease exiting the curve. This can be described by the spatial derivative of the radius of curvature along the motion path: $d\rho/ds < 0$ indicates entering a curve, and $d\rho/ds > 0$ indicates exiting a curve (see Appendix B for explanation of calculations). This trend appears strongly on the lemniscates with higher aspect ratio (#1,2,6), somewhat on the mid-range lemniscates (#3,5), and least on the wider, shorter lemniscate (#4). Lubricated sliding produces a similar trend with overall lower friction coefficient (Figure 5-3). Because the double Fermat spiral exhibits a gradual change in curvature, it exhibits the same trends, though less severely (Figure 5-4).

These data indicate that the extremes of friction coefficients from a single dry sliding cycle can be as low as 0.2 (broader curvature) and as high as 0.4 (tighter curvature). It follows that regions of the motion path where the pin dissipates the most energy (i.e. highest friction coefficient) should be the regions that would contribute more heavily to the overall wear of the system. The motion path is symmetric, but some of the areas of extreme friction are not mirrored; this could be due to uneven zeroing of the load cells before the test began.

Archimedes' Spiral Motion Path Friction Results

At 14,000 cycles, the average cycle friction is lowest for ever-increasing radius ($\mu = 0.199$), and is highest for ever-decreasing radius ($\mu = 0.231$) (Figure 5-5).

This is in agreement with the hypothesis that increasing radius of curvature will not produce as high friction as decreasing radius of curvature (increasing curve intensity). When average friction coefficient for each cycle is plotted versus time, it can be seen that the ever-decreasing radius of curvature reaches a steady state after the 14000 cycles which is slightly higher than the initial transient. Conversely, the ever-increasing radius of curvature continued to decrease to a value lower than the initial transient up to 14000 cycles (Figure 5-6).

Crossing Angle α

In these experiments, a crossing angle α can be calculated by taking the velocity vectors between consecutive points and seeing how they rotate as the motion advances. However, the plots do not yield useful information for this work because of the slight scatter in the position data collected. That scatter is magnified in velocity calculations, and does not show a clear track with friction coefficient at this juncture.

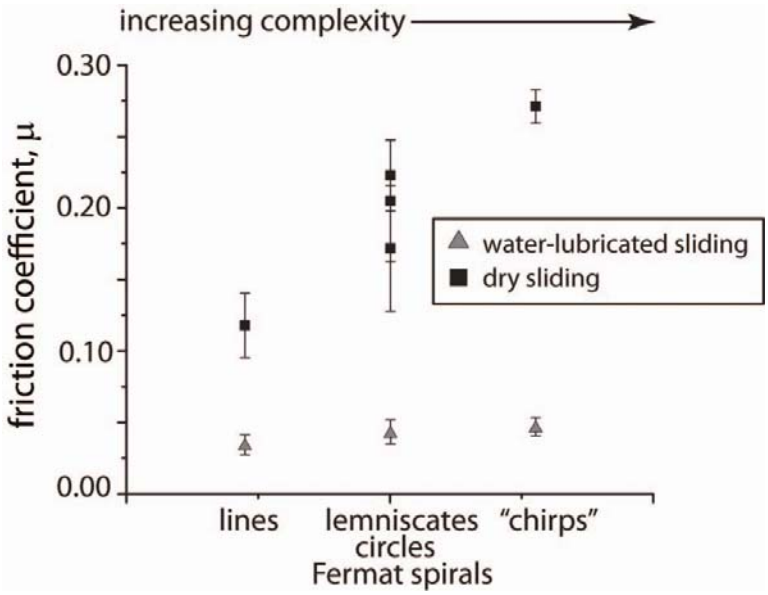

Figure 5-1. A summary of friction coefficients for a variety of geometries in dry and lubricated sliding.

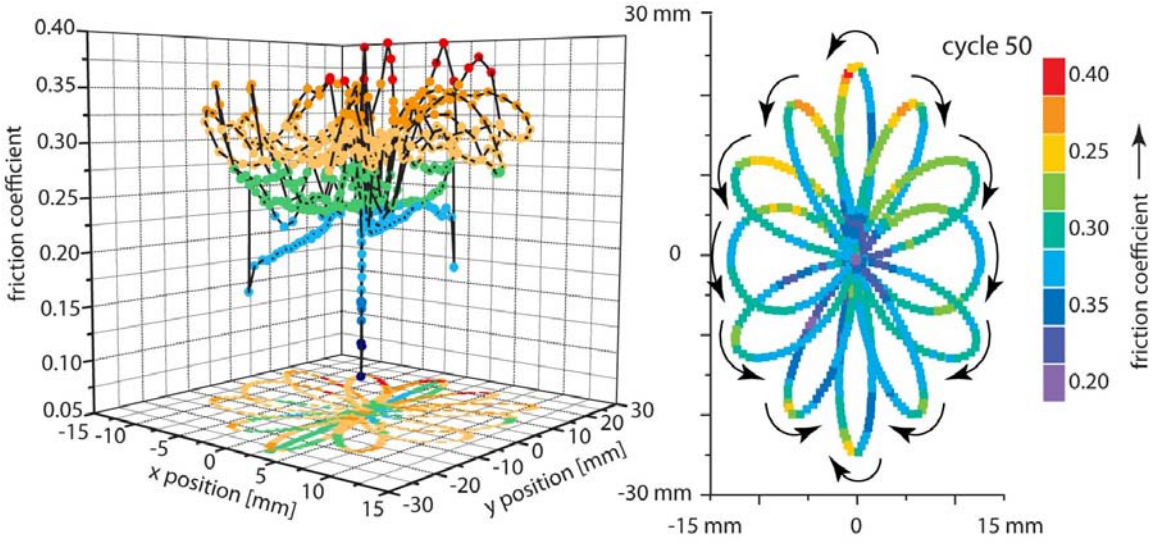

Figure 5-2. Friction coefficient as a function of wear track position for one cycle of the curvature-modulated "chirp" signal in dry sliding.

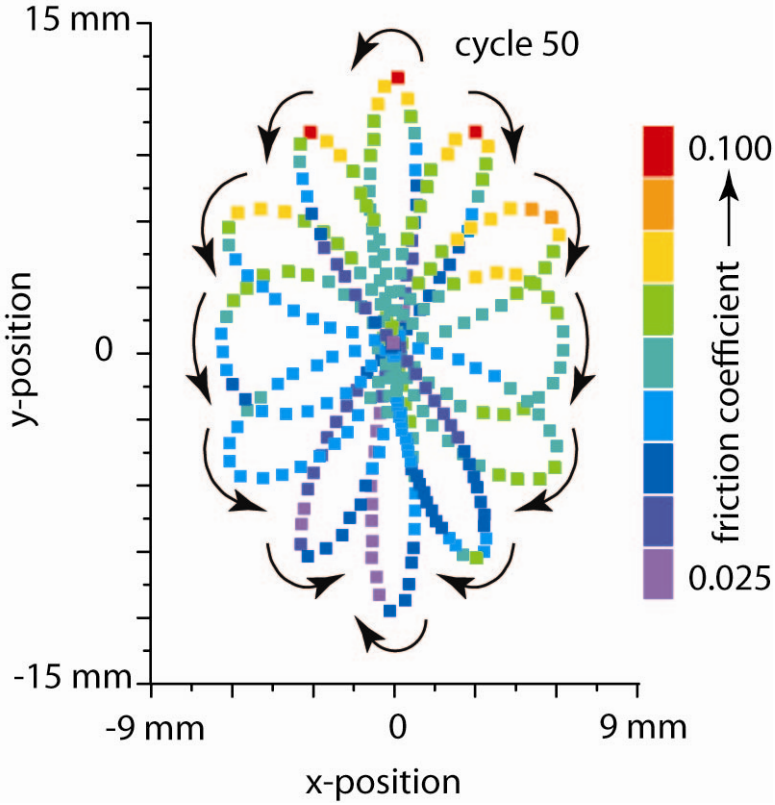

Figure 5-3. Friction coefficient as a function of wear track position for one cycle of the curvature-modulated “chirp” signal in lubricated sliding.

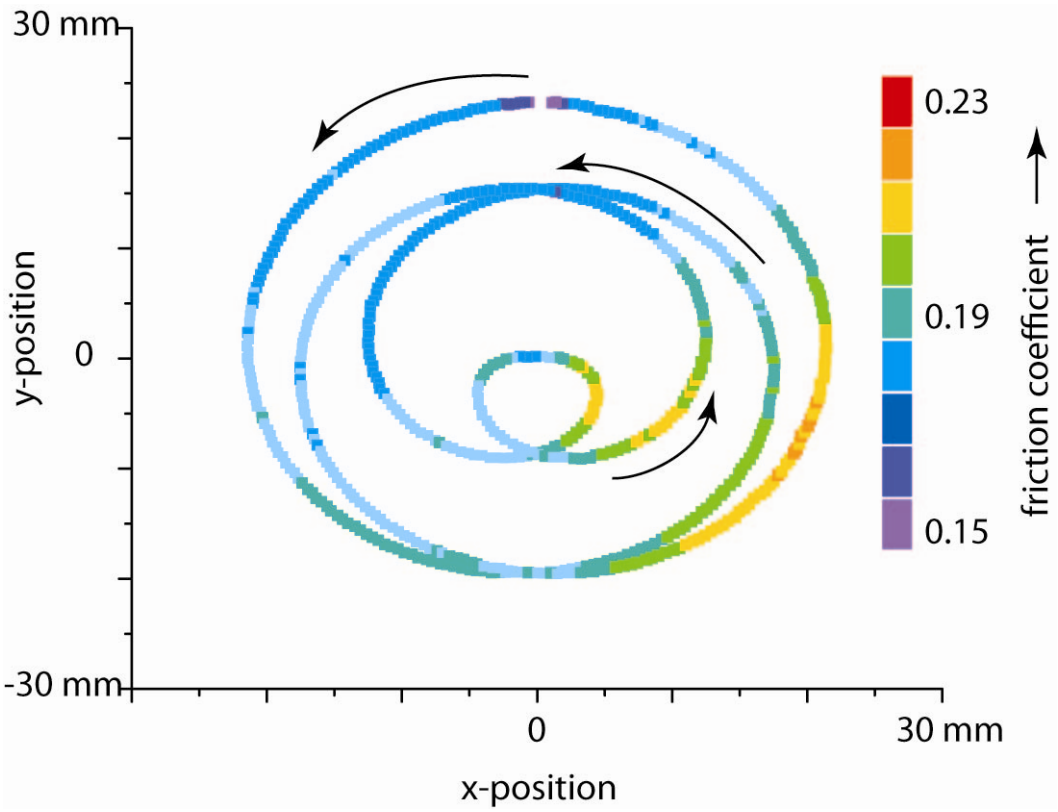

Figure 5-4. Friction coefficient in dry sliding as a function of wear track position for one cycle of the double Fermat spiral motion path.

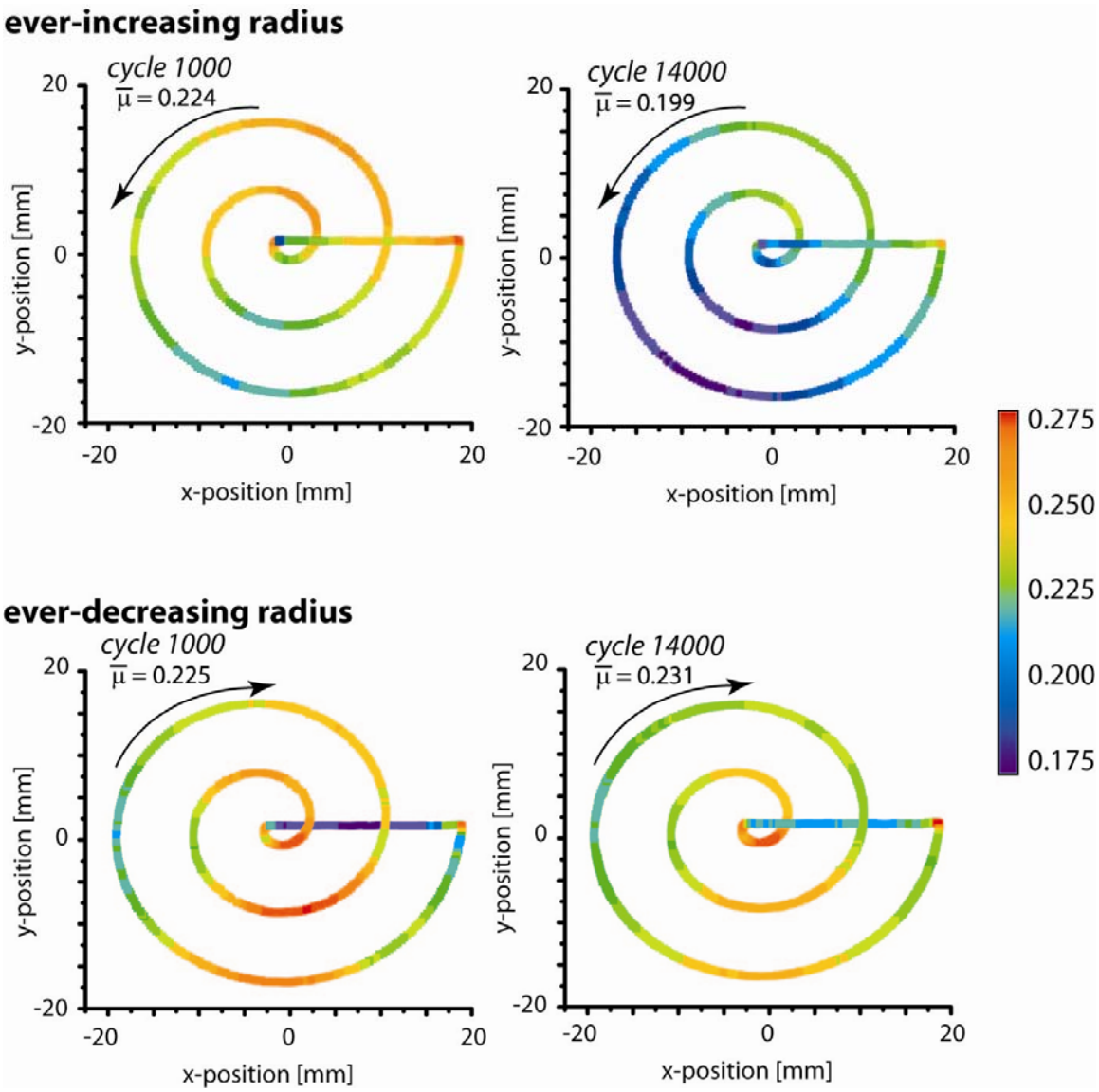

Figure 5-5. Friction coefficient as a function of wear track position for cycles 1000 and 14000 of the ever-increasing or ever-decreasing Archimedes' spirals.

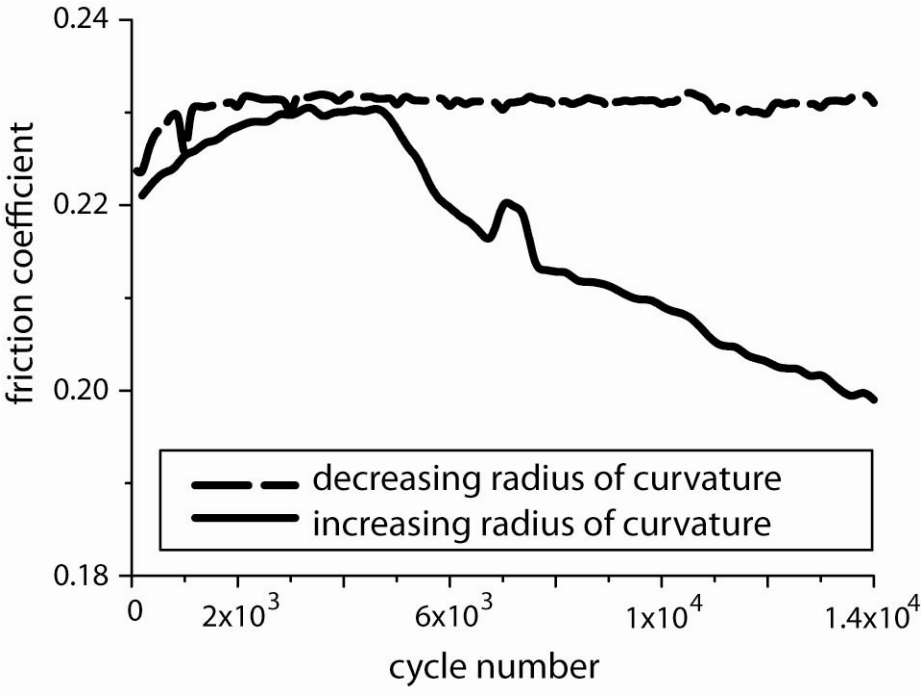

Figure 5-6. Friction coefficient as a function of cycle number of the ever-increasing or ever-decreasing Archimedes' spirals.

CHAPTER 6
DISCUSSION

This work has shown that friction coefficient measured *in situ* can be a key determinant as to the mechanisms of wear of UHMWPe in multidirectional sliding, specifically with respect to orientation of the surface in contact. As the derivative of radius of curvature increases, the steady-state friction is lower, and vice versa. This explains that there must be some orientation of the surface, and energy expended to cause that orientation. More energy is required to re-orient more quickly, so friction coefficient is overall higher. The size scale of these motion paths with respect to the size of the pin and the size of polyethylene molecule chains seems to fall in a range where these phenomena can be observed. There must exist a sliding motion length range for which orientation and re-orientation can take place, below which molecular interactions such as Van der Waals forces are too strong, and above which surface orientation is negligible. An estimate of this range of relevance would be on the order of micrometers up to meters.

Other authors have proved that UHMWPe wears more when there are more abrupt motion path changes; this confirms that the mechanisms of friction and wear are indeed related. Author Zmitrowicz has explored in detail a computational constitutive model where an initial velocity and motion path are prescribed, and then the friction trace calculated [28]. He concludes that for two ranges of curvature (possibly determined by parameters) the friction can either increase or decrease with increasing radius of curvature.

Crossing Angle Example: Circle Motion Path

To explore restrictions of the crossing angle effect on friction, a circular motion path was chosen to analyze. According to the reigning theory of surface elongation and perpendicular rupture, a circle with a smaller radius of curvature would result in higher friction because the surface would not have as much time to recover in the constant change of direction; the change of direction is more severe with circles of smaller radius. If it is true that small radii of curvature produce higher friction coefficient and higher crossing angle produce higher friction coefficients, then the analysis of curves must be consistent in one way: the motion paths must have constant velocity, and constant data acquisition speed to be accurately compared.

Constant velocity motion paths would allow the spacing of points on the path to be equal. Only when the spacing of points is equal can the angle of crossing be adequately assessed. For example, given a circle of radius S which has a 'small' radius of curvature, and a circle of radius L for a 'large' radius of curvature, the crossing angle would be the same value for both if both circles had the same amount of positions (Figure 6-1). (This would require either a different acquisition rate or different sliding velocity.) However, if the velocity remains constant, allowing an equal spacing of points for both circles, crossing angle varies with the radius of the circle (Figure 6-2).

Using the latter assumption, crossing angle can be calculated for a range of radii of curvature circles, and a relationship observed (Figure 6-3). These calculations used an initial case of radius of curvature ρ = 20 mm, 18 position points, and 6.95 mm between position points. Crossing angle α was solved for by changing the number of points on the circle until the distance d between points was equal for all circles. The relationship given here should not be specific to the circles chosen due to the non-dimensional group d/ρ,

which is the distance between points divided by the radius of the circle motion path in question. The power fit with exponent 1.025 indicates that there is a nearly linear relationship between these two parameters. If there is a definitive relationship between crossing angle and friction coefficient that can be verified empirically, friction coefficient could be predicted for each circle, as well as the friction rise due to the change in size of the circular motion path.

Friction Rise Predictions with Crossing Angle

Dr. Wang's theory as described earlier relates a change in friction coefficient to the rate of wear of UHMWPe, but he does not allow his directional energy equations to inform or quantify that change. The work in each sliding direction is defined by integrating the friction force times velocity over the course of time, to obtain independent equations in the x-direction (elongation), and y-direction (rupture) (Equation 2, Equation 3). The directions are different because of the dependence on the cross-shear angle, α.

$$\Delta W_x = \frac{2\mu P v}{\omega}\left(\alpha + \frac{\sin(2\alpha)}{2}\right) \qquad \text{Equation 2}$$

$$\Delta W_y = \frac{2\mu P v}{\omega}\left(\alpha - \frac{\sin(2\alpha)}{2}\right) \qquad \text{Equation 3}$$

From the friction coefficient proportionality to the work in each direction, one can predict the friction coefficient rise in a single direction based on the rise in work in that direction (a function of the turn angle from the previous path). Taking the ratio of the work in the perpendicular directions gives a ratio based on the cross-shear angle (Equation 4). This is a relation of the rupture work to the elongation work.

$$\frac{\Delta W_y}{\Delta W_x} = \frac{\left(\alpha - \frac{\sin(2\alpha)}{2}\right)}{\left(\alpha + \frac{\sin(2\alpha)}{2}\right)} \qquad \text{Equation 4}$$

It is predicted that there are two components to the friction coefficient: a sort of established, "steady-state" friction coefficient in the initial, chain-elongation sliding direction, μ_x, and a higher friction coefficient in the chain-rupture direction, μ_y. It is assumed that more work is required to rupture a chain than to elongate it. A general relationship between friction, work, and directionality can be surmised from Equation 4 (Equation 5). Simplifying will give us an expression for friction coefficient based on the single-direction friction coefficient and the ratio of work based on turning angle (Equation 6).

$$\frac{\mu_y}{\mu_x} \propto \frac{\Delta W_y}{\Delta W_x} = \frac{\left(\alpha - \frac{\sin(2\alpha)}{2}\right)}{\left(\alpha + \frac{\sin(2\alpha)}{2}\right)} \qquad \text{Equation 5}$$

$$\mu = \mu_x \left(\frac{\Delta W_y}{\Delta W_x} + 1\right) \qquad \text{Equation 6}$$

This model predicts a higher coefficient of friction for great cross-shear angles, with the highest values in the rupture direction being equal to the initial, elongation direction friction coefficient. The maximum overall friction coefficient is $\mu_{\max} = 2C\mu_x$, where C is an arbitrary constant. Figure 6-4 gives the change in friction coefficient as a function of cross-shear angle for various initial friction coefficients, μ_x, when C = 1.

For each of the lemniscates of the chirp motion path, α both increases up to π radians and decreases back to zero. Figure 6-5 shows how the friction traces compare when plotted against the calculated crossing angle for C = 1. There is no strong evidence

that friction coefficient increases up to twice as much as its starting value at a crossing angle of 90 degrees, but it does increase slightly. The discrepancy can be attributed to the path continually changing motion, which may not allow for a fully developed "elongation" portion and therefore no consistent base friction coefficient from which to increase, or measure that increase.

The theoretical rise in friction is not currently quantifiable and does not correlate well enough to empirical data to apply it to shapes such as the circles discussed previously, but these calculations are indicative that with further thought, reasonable relationships can be deduced from relevant and careful testing.

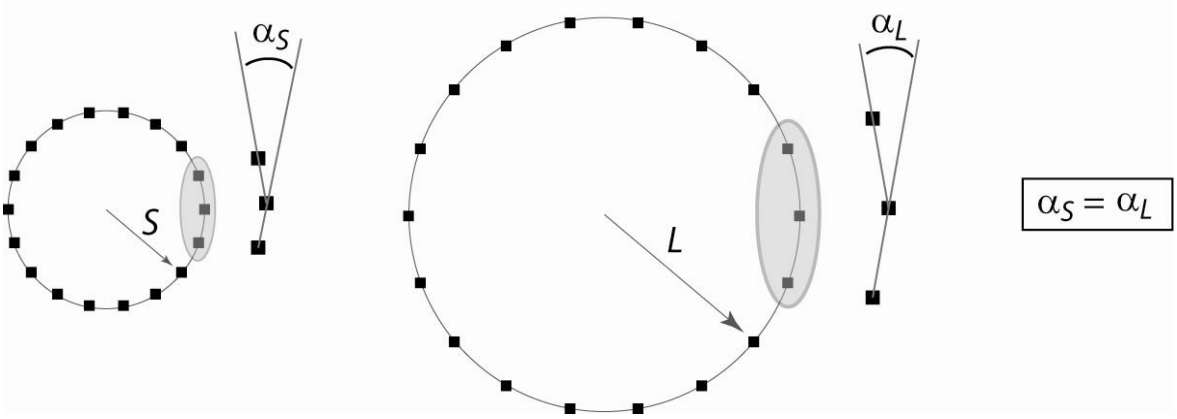

Figure 6-1. Schematic showing that α is the same for two circles of different sizes ($\rho=S$, $\rho=L$) because they contain the same number of position points.

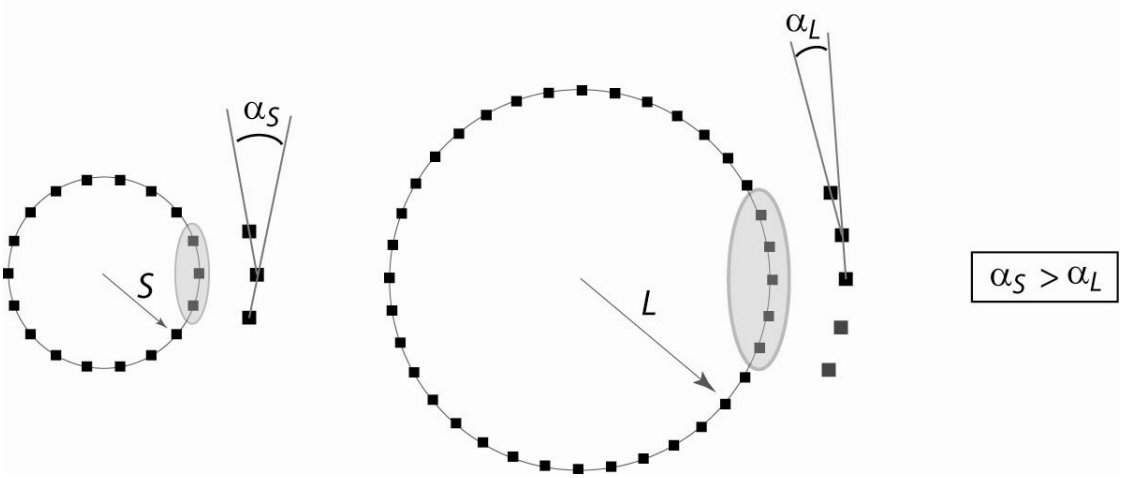

Figure 6-2. Schematic showing that α is different for two circles of different sizes ($\rho=S$, $\rho=L$) because they have constant velocity (different number of position points).

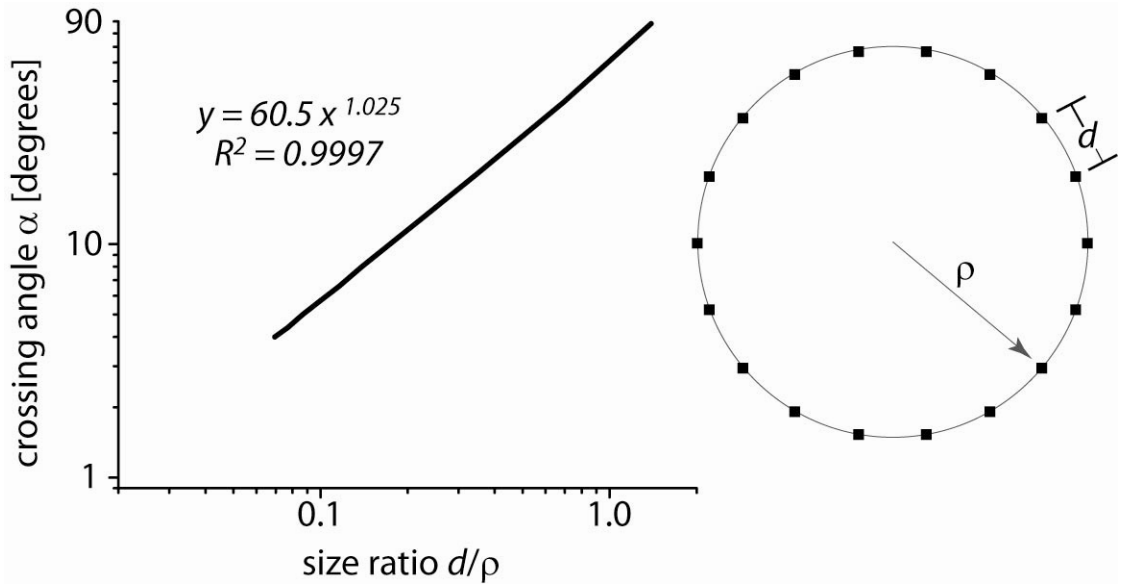

Figure 6-3. Plot of size ratio d/ρ versus crossing angle α produced.

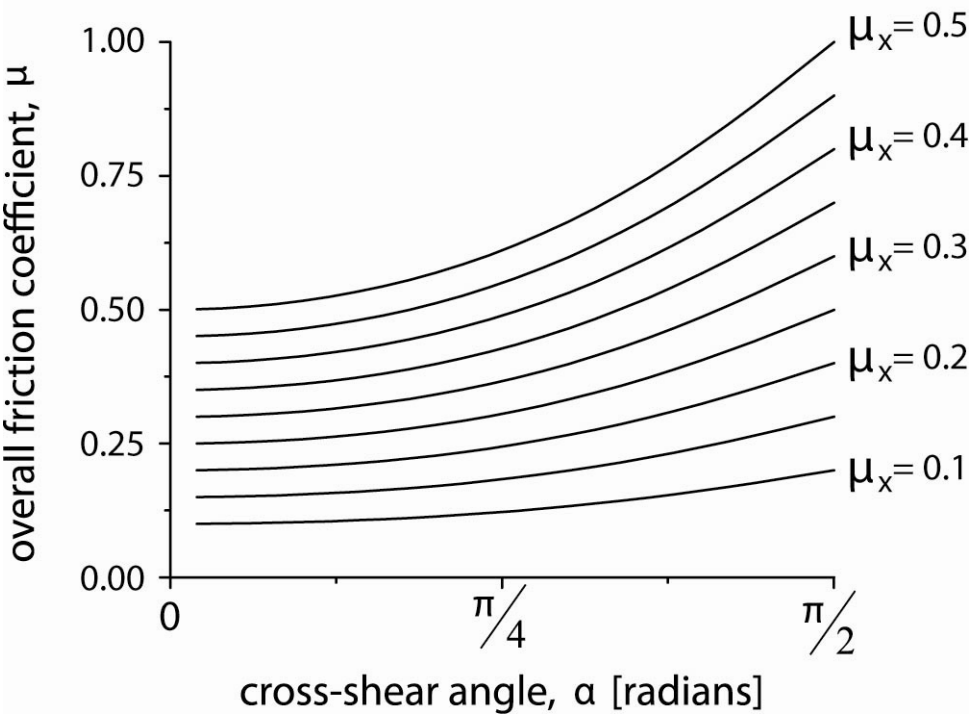

Figure 6-4. Friction coefficient rise predictions for base friction coefficients μ_x from 0.1 – 0.5 over the course of α from 0 – π radians.

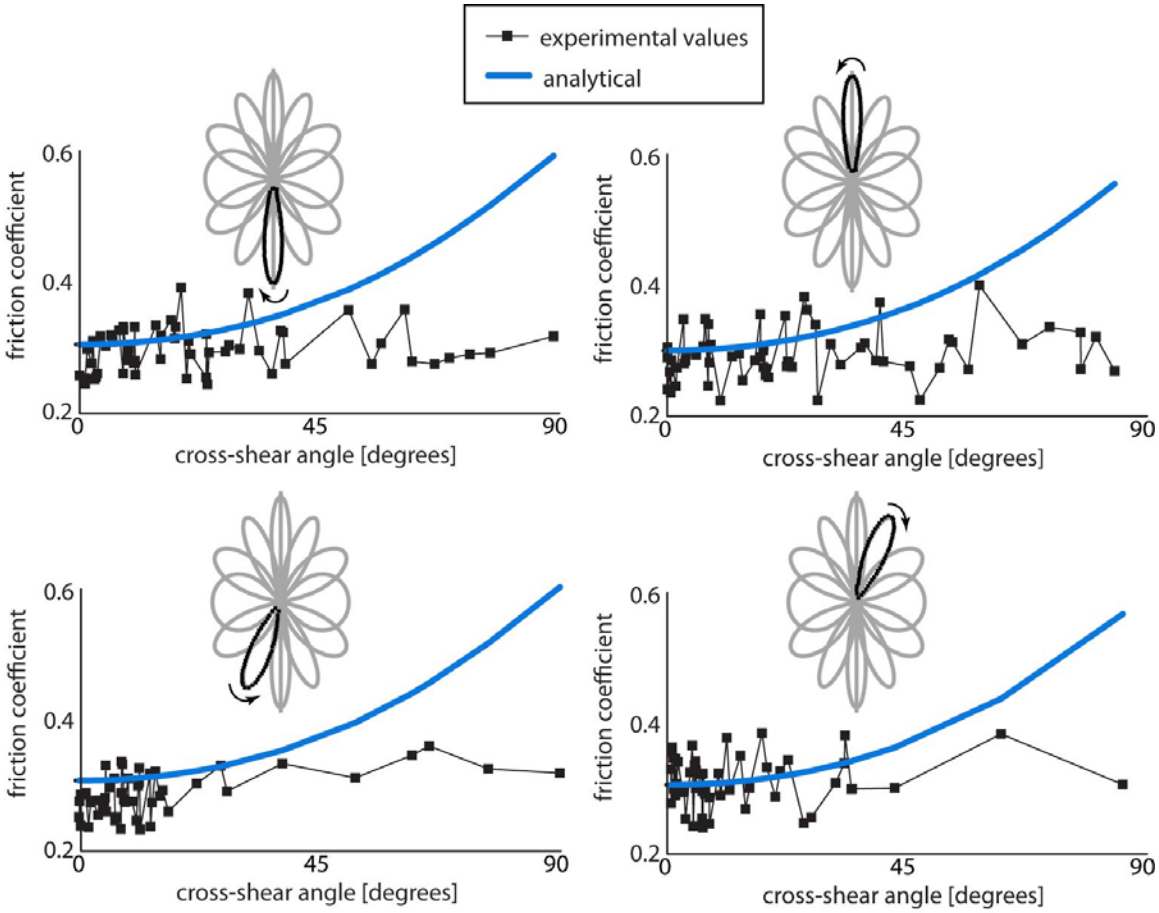

Figure 6-5. Experimental and theoretical friction coefficient plotted versus crossing angle α for selected lemniscates of the dry sliding chirp motion path.

CHAPTER 7
CONCLUSION

A multi-directional tribometer with the capabilities of uniform-velocity and uniform-pressure motion paths has been designed and constructed. It has been used to run a variety of motion paths with the aim of analyzing the resulting friction with the path parameters such as changes in curvature. It has been shown that when all other parameters remain constant, friction coefficient of UHMWPe in multi-directional sliding is affected by changes of curvature in the motion path. The chirp motion path with multiple passes of increasing and decreasing radius of curvature was run, and the highest friction is seen at times when the change of radius of curvature is negative ($d\rho/ds < 0$). Friction tends to increase with $d\rho/ds < 0$ and tends to decrease with $d\rho/ds > 0$. Due to size scales, this suggests that surface orientation is dependent upon the length over which fibrils can align and the energy required to do so.

Based on hypotheses of the surface orientation of UHMWPe, it has been shown that there should be a quantifiable rise in friction each time the path motion vector changes in direction by some angle α. Because the experimental did not correlate well to the expected rise in friction coefficient for various lemniscates in our chirp motion path, more work is needed in modeling the rise in friction with changes in the motion path to quantify how friction can be a predictor of wear, in conjunction with alternate methods of calculating α.

The ramifications of using *in situ* friction traces in current theories of surface elongation and even unified wear theories are sizable. Limits can be applied to the theory

of surface orientation with respect to the pin size, sliding length, and paths necessary to enact the phenomenon. More severe motions on the wear path can be correlated to specific locations where higher wear might take place, rather than a general association of the two. Also, some functionality of friction coefficient with crossing angle can be inserted into unified wear theories rather than simplified assumptions of constant friction through an entire complex motion path.

APPENDIX A
WEAR CALCULATIONS

Wear calculations are done using gravimetric analysis of polymer samples. This means that volume loss is calculated from a measured mass loss (scale resolution down to 10 μg). Material comparison is made by the wear rate, rather than wear over a given sliding distance or time, which allows for flexibility of measurements systems (Figure A-1).

Wear rate is designated by k, and is the volume lost divided by the normal force applied times the distance of sliding (Equation 7).

$$k = \frac{V_{lost}}{F_n d} \qquad \text{Equation 7}$$

The volume lost is calculated by taking the measured mass lost and dividing by the density of sample (Equation 8), which is defined by the initial mass divided by the initial volume of the sample (Equation 9). Sliding distance is constituted by the sliding distance of each cycle and the total number of cycles (Equation 10).

$$V_{lost} = \frac{\Delta m}{\rho_{sample}} \qquad \text{Equation 8}$$

$$\rho_{sample} = \frac{4m_0}{\pi D^2 L} \qquad \text{Equation 9}$$

$$d = S * N \qquad \text{Equation 10}$$

When all these variables are combined, wear rate is given by Equation 11.

$$k = \frac{\Delta m \pi D^2 L}{4 F_n S N m_0} \qquad \text{Equation 11}$$

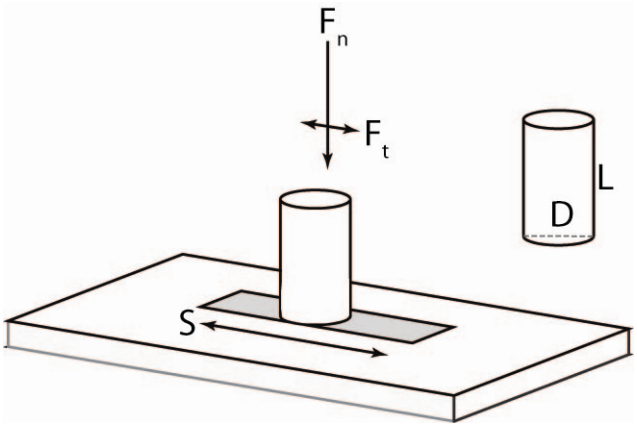

Figure A-1. A schematic describing the dimensions and forces used to calculate wear rate. Courtesy of Dave Burris.

APPENDIX B
RADIUS OF CURVATURE CALCULATION METHOD

The common radius of curvature for three points on a continuous curve is calculated by find the circumcircle of the triangle made up of those three points. The distance between any point and the circumcenter of that circle is the radius of curvature, ρ (Figure B-1).

First, the lengths of the legs (*a, b, c*) of the triangle *IJK* are calculated using the distance formula (Equation 12). The first intermediate step is to calculate a parameter of the triangle *s*, which is a function of the leg lengths (Equation 13). From this parameter and the lengths, the radius of curvature is calculated (Equation 14).

$$a = \sqrt{\left(x_i - x_j\right)^2 + \left(y_i - y_j\right)^2} \qquad \text{Equation 12}$$

$$s = \frac{a+b+c}{2} \qquad \text{Equation 13}$$

$$\rho = \frac{abc}{4\sqrt{s\left(s-a\right)\left(s-b\right)\left(s-c\right)}} \qquad \text{Equation 14}$$

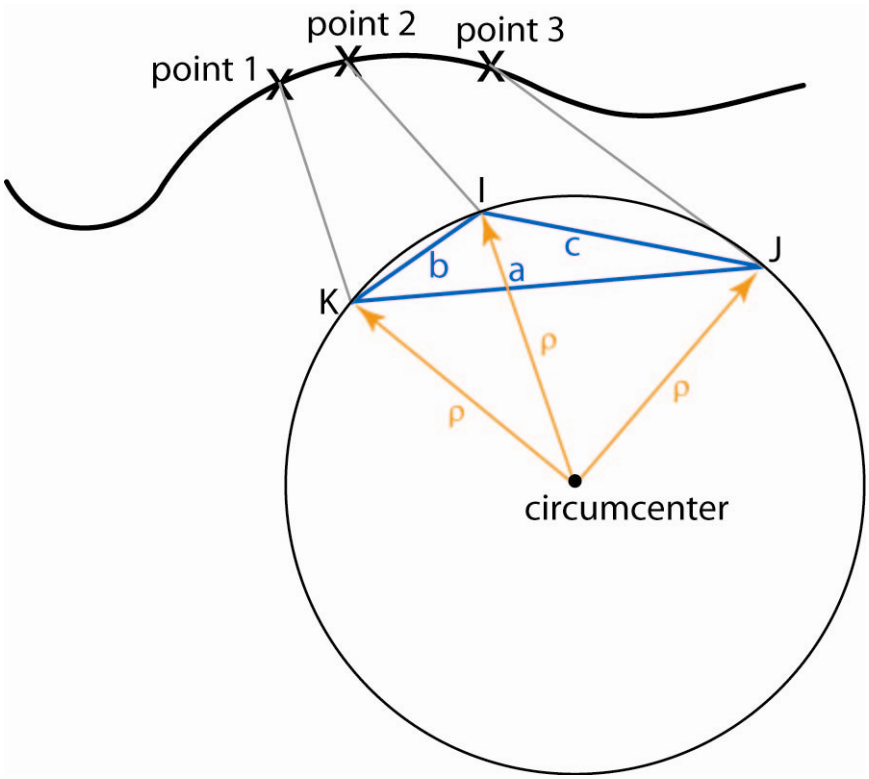

Figure B-1. Schematic of curve-fitting a circle between three points on a continuous curve.

LIST OF REFERENCES

1. Bennett, D., Orr, J., Beverland, D.,Baker, R., The Influence of Shape and Sliding Distance of Femoral Head Movement Loci on the Wear of Acetabular Cups in Total Hip Arthroplasty. Proceedings of the Institution of Mechanical Engineers Part H—Journal of Engineering Medicine, 2002. 216(H6): p. 393-402.

2. Bragdon, C.R., Goetz, D.D., Jasty, M., Elder, J.R., Variables Affecting the Wear of Polyethylene Acetabular Components, from AAHKS Fifth Annual Meeting Proceedings. The Journal of Arthroplasty, 1996. 11(2): p. 229.

3. Fregly, B., Sawyer, W., Harman, M., Banks, S., Computational Wear Prediction of a Total Knee Replacement from *in vivo* Kinematics. Journal of Biomechanics, 2005. 38(2): p. 305-314.

4. Hamilton, M., Sucec, M., Fregly, B., Banks, S., Sawyer, W., Quantifying Multidirectional Sliding Motions in Total Knee Replacements. Journal of Tribology—Transactions of the ASME, 2005. 127(2): p. 280-286.

5. Laurent, M., Johnson, T., Yao, J., Blanchard, C., Crowninshield, R., In Vitro Lateral versus Medial Wear of a Knee Prosthesis. Wear, 2003. 255: p. 1101-1106.

6. Gonzalez-Mora, V., Hoffmann, M., Chiesa, R., Cigada, A., Hampshire, J., Stroosnijder, M.F., Screening Wear Tester Versus Hip Joint Simulator: Results of UHMWPe Sliding against Different CoCrMo Counterfaces. Surface Engineering, 2003. 19(1): p. 45-50.

7. Hoffmann, A., Gonzalez-Mora, V., Chiesa, R., Cigada, A., Stroosnijder, M., Screening of Stabilized Crosslinked Polyethylene Using a Novel Wear Tester. Biomedical Materials and Engineering, 2002. 12(4): p. 387-395.

8. Kurtz, S., Pruitt, L., Jewett, C., Foulds, J., Edidin, A., Radiation and Chemical Crosslinking Promote Strain Hardening Behavior and Molecular Alignment in Ultra High Molecular Weight Polyethylene During Multi-Axial Loading Conditions. Biomaterials, 1999. 20(16): p. 1449-1462.

9. Shen, F., McKellop, H., Salovey, R., Morphology of Chemically Crosslinked Ultrahigh Molecular Weight Polyethylene. Journal of Biomedical Materials Research, 1998. 41(1): p. 71-78.

10. Turell, M., Bellare, A., A Study of the Nanostructure and Tensile Properties of Ultra-High Molecular Weight Polyethylene. Biomaterials, 2004. 25(17): p. 3389-3398.

11. Yao, J., Blanchet, T., Murphy, D., Laurent, M., Effect of Fluid Absorption on the Wear Resistance of UHMWPe Orthopedic Bearing Surfaces. Wear, 2003. 255: p. 1113-1120.

12. Wang, A., A Unified Theory of Wear for Ultra-High Molecular Weight Polyethylene in Multi-Directional Sliding. Wear, 2001. 248(1-2): p. 38-47.

13. Gevaert, M., LaBerge, M., Gordon, J., DesJardins, J., The Quantification of Physiologically Relevant Cross-Shear Wear Phenomena on Orthopedic Bearing Materials Using the Max-Shear Wear Testing System. Journal of Tribology—Transactions of the ASME, 2005. 127(4): p. 740-749.

14. Galvin, A., Kang, L., Tipper, J., Stone, M., Ingham, E., Jin, Z., Fisher, J., Wear of Crosslinked Polyethylene under Different Tribological Conditions. Journal of Materials Science—Materials in Medicine, 2006. 17(3): p. 235-243.

15. Muratoglu, O., Bragdon, C., O'Connor, D., Jasty, M., Harris, W., Gul, R., McGarry, F., Unified Wear Model for Highly Crosslinked Ultra-High Molecular Weight Polyethylenes (UHMWPe). Biomaterials, 1999. 20(16): p. 1463-1470.

16. Wang, A., Essner, A., Polineni, V., Stark, C., Dumbleton, J., Lubrication and Wear of Ultra-High Molecular Weight Polyethylene in Total Joint Replacements. Tribology International, 1998. 31(1-3): p. 17-33.

17. Burroughs, B., Blanchet, T., Factors Affecting the Wear of Irradiated UHMWPe. Tribology Transactions, 2001. 44(2): p. 215-223.

18. Saikko, V., Ahlroos, T., Wear Simulation of UHMWPe for Total Hip Replacement with a Multidirectional Motion Pin-on-Disk Device: Effects of Counterface Material, Contact Area, and Lubricant. Journal of Biomedical Materials Research, 2000. 49(2): p. 147-154.

19. Saikko, V., Calonius, O., Keranen, J., Effect of Slide Track Shape on the Wear of Ultra-High Molecular Weight Polyethylene in a Pin-on-Disk Wear Simulation of Total Hip Prosthesis. Journal of Biomedical Materials Research Part B—Applied Biomaterials, 2004. 69B(2): p. 141-148.

20. Joyce, T., Monk, D., Scholes, S., Unsworth, A., A Multi-Directional Wear Screening Device and Preliminary Results of UHMWPe Articulating against Stainless Steel. Bio-medical Materials and Engineering, 2000. 10(3-4): p. 241-249.

21. Sawae, Y., Murakami, T., Sawano, T., Noda, I., Shimotoso, T., Quantitative Evaluation of Wear Property of Polyethylene-on-Ceramic Sliding Pairs for Joint Prostheses in Multidirectional Sliding Test. Bioceramics 14, 2002. 218-2: p. 665-668.

22. Wang, A., Essner, A., Stark, C., Dumbleton, J., A Biaxial Line-Contact Wear Machine for the Evaluation of Implant Bearing Materials for Total Knee Joint Replacement. Wear, 1999. 229: p. 701-707.

23. Endo, M., Barbour, P., Barton, D., Fisher, J., Tipper, J., Ingham, E., Stone, M., Comparative Wear and Wear Debris under Three Different Counterface Conditions of Crosslinked and Non-Crosslinked Ultra High Molecular Weight Polyethylene. Bio-medical Materials and Egineering, 2001. 11(1): p. 23-35.

24. Marrs, H., Barton, D., Jones, R., Ward, I., Fisher, J., Doyle, C., Comparative Wear under Four Different Tribological Conditions of Acetylene Enhanced Cross-Linked Ultra High Molecular Weight Polyethylene. Journal of Materials Science—Materials in Medicine, 1999. 10(6): p. 333-342.

25. Fisher, J., McEwen, H., Tipper, J., Galvin, A., Ingram, J., Kamali, A., Stone, M., Ingham, E., Wear, Debris, and Biologic Activity of Cross-Linked Polyethylene in the Knee - Benefits and Potential Concerns. Clinical Orthopaedics and Related Research, 2004(428): p. 114-119.

26. Turell, M., Wang, A., Bellare, A., Quantification of the Effect of Cross-Path Motion on the Wear Rate of Ultra-High Molecular Weight Polyethylene. Wear, 2003. 255: p. 1034-1039.

27. Turell, M., Friedlaender, G., Wang, A., Thornhill, T., Bellare, A., The Effect of Counterface Roughness on the Wear of UHMWPe for Rectangular Wear Paths. Wear, 2005. 259: p. 984-991.

28. Zmitrowicz, A., Models of Kinematics Dependent Anisotropic and Heterogeneous Friction. International Journal of Solids and Structures, 2006. 43: p. 4407-4451.

BIOGRAPHICAL SKETCH

Alison Dunn first gained an education of cultures by moving around frequently until starting at the University of Florida in August of 2000. She earned a Bachelor of Science degree in mechanical engineering in December of 2004. She has received various awards including participation in the University Scholars' Program and the Caterpillar Scholarship from the Society of Women Engineers. Upon obtaining a Master of Science, she plans to join the Peace Corps and eventually work for a biomedical company or technical instrumentation company.